

Freezing Point Depression Method for Hydrate Monitoring

By

Muhammad Bukhari bin Abdul Jalil

6412

**Dissertation submitted in partial fulfillment of
the requirements for the
Bachelor of Engineering (Hons)
(Mechanical Engineering)**

DECEMBER 2008

**Universiti Teknologi PETRONAS
Bandar Seri Iskandar
31750 Tronoh
Perak Darul Ridzuan**

CERTIFICATION OF APPROVAL


Freezing Point Depression Method for Hydrate Monitoring

by

Muhammad Bukhari bin Abdul Jalil

A project dissertation submitted to the
Mechanical Engineering Programme
Universiti Teknologi PETRONAS
in partial fulfilment of the requirement for the
BACHELOR OF ENGINEERING (Hons)
(MECHANICAL ENGINEERING)

Approved by,



(Pn Mazlin Idress)

UNIVERSITI TEKNOLOGI PETRONAS

TRONOH, PERAK

December 2008

CERTIFICATION OF ORIGINALITY

This is to certify that I am responsible for the work submitted in this project, that the original work is my own except as specified in the references and acknowledgements, and that the original work contained herein have not been undertaken or done by unspecified sources or persons.



MUHAMMAD BUKHARI BIN ADBUL JALIL

ABSTRACT

This report gives an extensive review on the overall project works which include background of study, problem statement, significance of study, objectives and scope of work, literature review, methodology, and results and discussion. The introduction section describes the overview of natural gas hydrates as pipeline plugging and the importance of hydrate monitoring method. The critical problem associated with injecting thermodynamic inhibitors to prevent hydrate formation is adequate amount of thermodynamic inhibitors to ensure the operating conditions falls out of the hydrate stability zone and at the same time optimize the operating costs. The primary objective of this project is to determine the suitable operating pressure and temperature limits for deepwater fields producing 50 - 65 mole percent of methane (CH_4) using Freezing Point Depression method. The literature review section provides the theoretical aspect of the work and some correlations that will be used in accordance to the FPD method. The methodology section discusses the work need to be done to accomplish the project objectives. There are 3 main tasks in this work which are experimental, correlations and simulation. The experimental procedures and the prototype equipment used will be discussed at length in Chapter 3. Results from experimental work and correlations are presented in the Chapter 4. These experimental data showed high degree of precision which indicates that this method is applicable and practical. The hydrate phase boundary obtained using the correlations are presented in the same chapter. These results are compared with simulation results using PVT-sim. The overall outcome of the project is a graphical representation of the suitable operating conditions for reservoir fluid composed of 50 – 65 mol% of methane. The limitations of the prototype equipment will also be discussed in the same chapter. All of the information provided in this report is concluded in the conclusion section.

ACKNOWLEDGEMENT

First of all, I would like to thank God for granting me the strength and determination to complete the project within the time limit. I would also like to express my deepest appreciation to my supervisor Pn Mazlin Idress who has tirelessly guided me throughout the year. Not to forget her kind support and assistance during the planning phase of the project. I would like to extend my deepest gratitude towards Dr Ahmad Majdi b Abdul Rani who has supervised me in terms of the mechanical elements in the project.

Special thanks to Pn Zahidah Md Zain from PETRONAS Research Sdn Bhd (PRSB) for her kind support and advice throughout the project. I would also like to thank any individuals or organizations which were involved directly or indirectly to assure the success of this project.

CONTENT

CERTIFICATION OF APPROVAL	i
CERTIFICATION OF ORIGINALITY	ii
ABSTRACT	iii
ACKNOWLEDGEMENT	vi
CHAPTER 1: INTRODUCTION	1
1.1 Background of Study.....	1
1.2 Problem Statement	2
1.3 Significance of Study	3
1.4 Project Objectives and Scope of Work	3
CHAPTER 2: LITERATURE REVIEW	5
2.1 Natural Gas Hydrates	5
2.2 Freezing Point Depression Method	6
2.3 Correlations	7
CHAPTER 3: METHODOLOGY	11
CHAPTER 4: RESULTS AND DISCUSSION.....	19
4.1 Base Case Scenario	19
4.2 Freezing Point Depression Method	20
4.3 Correlations	26
4.4 Simulation	31
4.5 Suitable Operation Conditions	33
CHAPTER 5: CONCLUSION	37
REFERENCES	38
APPENDICES	39

LIST OF FIGURES

Figure 1	General form of hydrate phase boundary	5
Figure 2	Hydrate suppression temperature for methane hydrates versus freezing point depression temperature in the presence of aqueous solutions containing salt and/or organic inhibitor	9
Figure 3	Step-by-step Methodology	11
Figure 4	Correlation used to developed hydrate phase boundary with the presence of distilled water	12
Figure 5	Schematic diagram of Freezing Point Depression prototype equipment	15
Figure 6	Temperature control system of the prototype equipment.....	16
Figure 7	Base case hydrate phase boundary for Field A and Field B.....	19
Figure 8	Exported data from temperature acquisition software	20
Figure 9	FPD result for Field A with 15 wt% Methanol (FA15MV1R1)	21
Figure 10	Prediction of hydrate phase boundary using correlation – Field A with methanol inhibition.....	27
Figure 11	Prediction of hydrate phase boundary using correlation – Field A with ethylene glycol inhibition	27
Figure 12	Prediction of hydrate phase boundary using correlation – Field B with methanol inhibition.....	28
Figure 13	Prediction of hydrate phase boundary using correlation – Field B with ethylene glycol inhibition	28
Figure 14	Comparison of Methanol and Ethylene Glycol towards shifting hydrate phase boundary for Field A	30
Figure 15	Comparison of Methanol and Ethylene Glycol towards shifting hydrate phase boundary for Field B.....	30
Figure 16	Graphical results of simulation using PVT-sim	31
Figure 17	Graphical comparisons between results from FPD method and PVT-sim.....	33

Figure 18 Graphical representation of operation pressure and temperature limits for reservoir producing 50 - 65 mol% of methane	35
--	----

LIST OF TABLES

Table 1 Salt used to prepare synthetic produced water sample.....	13
Table 2 Samples prepared for analysis using Freezing Point Depression method	14
Table 3 Freezing Point Depression results for Field A	22
Table 4 Freezing Point Depression results for Field B	23

CHAPTER 1

INTRODUCTION

1.1 BACKGROUND STUDY

In the mid 1930's, Hammerschmidt (1939) discovered natural gas hydrates as pipeline plugs or as a flow assurance problem in the oil and gas industry. He determined that hydrates were blocking gas transmission lines, frequently at temperatures above the ice point. This discovery was pivotal in causing a more pragmatic interest in gas hydrates, and shortly thereafter led to the regulation of the water content in natural gas pipelines (Sloan, 1998). The detection of hydrates in pipelines is a milestone marking both the importance of hydrates to industry and the beginning of the modern research era.

Hydrate formation and accumulation in pipelines and surface facilities may lead to interruption of production which can be considered a significant economic risk to the industry. Further plugging could also result in damage to facilities and risk personnel safety. According to Chatti and co-workers, the plug formed from hydrates can also behave as a projectile that destroys the pipe when pressure difference between the upstream and downstream sections increases (Chatti et al, 2005). These major consequences have increased the significance of hydrate monitoring to the oil and gas industry. There are few methods available for hydrate monitoring which include Freezing Point Depression, Conductivity-Velocity and Water Activity (Najibi et al., 2006; Mohammadi et al, 2007a, b).

Hydrate monitoring methods can be done in laboratory experiments to determine the hydrate safety margin. Hydrate monitoring is usually applied in conjunction with deepwater production operations and natural gas transmission using deepwater pipelines. The current research trend has started to focus on hydrate monitoring methods as online applications whereby these methods can be done from time to time.

1.2 PROBLEM STATEMENT

The primary purpose of hydrate monitoring is to predict the adequate amount of thermodynamic inhibitors to be injected into the system to prevent hydrate formation and accumulation. Hydrate monitoring is also important to minimize inhibition cost and ensure environmental safety. As far as the world is concern, injecting excessive inhibitor will increase operations cost and causes significant effect to the environment. It must also important to note that, under-inhibited system will cause the hydrate to form at the walls and resulting in a much greater effect than not injecting inhibitor at all (Sloan, 1998).

The reservoir fluid composition of reservoir and the operation pressure and temperature changes from time to time thus affecting the degree of inhibition required. Some production operators tend to inject up to 50 wt% of methanol into the system as hydrate prevention method without prediction of the required adequate amount. This may result in excess chemical injected and thus increase operational cost. It should be noted that with a proper prediction method, we could possibly prevent hydrate formation, minimize operational cost and reduce environmental effect.

In some cases where there is high risk of hydrate formation due to the pressure and temperature conditions, the usage of thermodynamic inhibitors to shift hydrate

phase boundary is not economical. Up to 60 wt% of inhibitors need to be injected to assure that the production is carried out outside the hydrate stability zone.

Currently, there are limited techniques which can be used to monitor hydrate in the pipeline to ensure sufficient volume of thermodynamic inhibitor is injected into the system. There are plenty correlations developed by researchers in their literature, but most of them are theoretical or empirical equations which have limited applicability. In this work, a physical (experimental) technique with a reliable correlation is used as a method for hydrate monitoring.

1.3 SIGNIFICANCE OF STUDY

This study integrates experimental, correlations and simulation work to achieve its objectives. A case study is being done with two reservoir data which include produced water sample composition and reservoir fluid composition. Based on the case study done using these data from Field A and Field B, hydrate phase boundary curve can be determined for reservoir producing moderate amount of methane. Apart from the natural inhibition of salt content in the produced water, the effect of injecting thermodynamic inhibitors will be studied as to provide more flexible conditions for the operation. The hydrate phase boundary curve for uninhibited and inhibited system together with operational pressure and temperature data is used to predict hydrate formation in deepwater operations. The outcome of the study can also be used as a baseline for predicting hydrate phase boundary in deepwater operations. The correlations and simulation used in this study can be used to compare the results from the experiments. This study is significant to the oil and gas industry in providing a proper method of predicting hydrate phase boundary for hydrate monitoring.

1.4 OBJECTIVES AND SCOPE OF WORK

The objectives of this project are:

1. To determine the suitable operating pressure and temperature limits for deepwater fields producing 50 - 65 mole percent of methane (CH_4) using Freezing Point Depression method.
2. To investigate the performance of methanol and ethylene glycol towards shifting hydrate phase boundary.

To achieve the objectives stated above, several works has been planned which include a case study using real data from two fields. The scope of work for the 1st semester is:

1. Literature review
2. Freezing Point Depression method
3. Prediction of hydrate phase boundary using correlations.

In the 2nd semester the scope of work is prediction of hydrate phase boundary using simulation. These simulation results will be compared to the results obtained from FPD method. Based on the work done, the suitable pressure and temperature conditions for field producing moderate amount of methane is determined.

CHAPTER 2

LITERATURE REVIEW

2.1 NATURAL GAS HYDRATES

Hydrate is defined as a crystalline solid which consists of gas molecules surrounded by a cage of water molecules. Most low molecular weight gases and several low carbon-number hydrocarbons form hydrates at certain temperature and pressure condition. Gas hydrates are similar to ice but they are unstable when empty, collapsing into conventional ice crystal structure. They are stabilized by the inclusion of appropriately sized molecules between them. Pressure and temperature are the main factors that control the stability of hydrates.

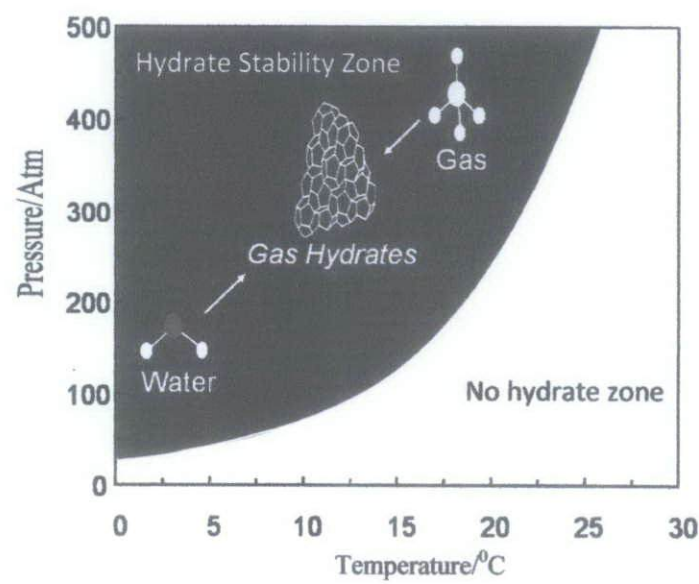


Figure 1: General form of hydrate phase boundary

From *figure 1*, it can be clearly seen that gas hydrates form at low temperature and high pressure condition. At higher pressures, gas hydrates are stable at temperatures up to 25⁰C. Thus it could be understood that, gas hydrates are likely to form in deepwater operations. It must be noted that the hydrate phase boundary shown in *figure 1* is only a general form. Slight difference may be encountered when the composition of gas is different.

Methane, among others, can be considered as the major hydrate former in reservoir fluid. The concentration of methane in reservoir fluid may have a great effect in the hydrate phase boundary where reservoir fluid with higher concentration of methane have a higher risk of hydrate formation compared to reservoir fluid with lower concentration of methane.

Thermodynamic inhibitors have long been used in the industry to shift hydrate phase boundary to a lower temperature and/or higher pressure conditions. This effort is being done to ensure the expected operation temperature and pressure falls out of the hydrate phase boundary.

2.2 FREEZING POINT DEPRESSION METHOD

Freezing Point Depression (FPD) method utilizes the feasibility of predicting the hydrate suppression temperatures of fluids from freezing point depression data of aqueous solutions containing different concentrations of salt and/or non-hydrate forming organic inhibitor (Najibi et al., 2006). FPD method should be done whenever thermodynamic inhibitors are likely to be used as a method of hydrate prevention. The data from FPD method is then investigated by using correlations. FPD considers only the changes in the freezing point of aqueous solution, and there is no need for the analytical composition of the aqueous solution. The measurement of the freezing point for the aqueous phase is much easier than measuring the hydrate dissociation point (Najibi et al., 2006). Thus FPD can be seen as an opportunity to

reduce experimental time and cost. Furthermore, freezing point of ice can also be achieved in standard laboratory equipment making it possible for plenty of iteration.

2.3 CORRELATIONS

Hammerschmidt equation was widely used in the oil and gas industry since decades ago to predict the depression temperature of hydrates formation in the existence of thermodynamic inhibitors. Hammerschmidt equation is an empirical equation and not applicable for the inhibitors that are not tested (Ming Wu et al., 2007). The limitation of this equation is that it neglects the content of inhibitor that is evaporated or in the saturated gas phase thus making it unsuitable for application of methanol concentration more than 25 wt%.

$$\Delta T = \frac{Kx}{M(100-x)} \quad (1)$$

In *Equation 1*, ΔT represents the temperature lowering for the formation of hydrate, K is a constant specific to each inhibitor, M is the molecular weight of the inhibitor; x is the mass concentration of the inhibitor.

Nielsen and Bucklin has founded that ice freezing point depression and hydrate formation temperature can be linearly related (Nielsen and Bucklin, 1983). The value of hydrate formation temperature varies from 0.6 to 0.7 of the ice freezing point depression and it depends on the enthalpy of formation of the hydrate.

$$\Delta T_{\text{hydrate}} = (\text{constant})\Delta T_{\text{ice}} \quad (2)$$

Østergaard et al. (2000) has developed a correlation to predict hydrate-free zone of reservoir fluids, from black oil to lean natural gas. The method correlates the

hydrate dissociation pressure against the specific gravity and the concentration of the hydrate-forming components in the fluid, as well as the temperature of the system. The effect of nitrogen and carbon dioxide on the hydrate-free zone has also been taken into account. The correlation has been developed using hydrate phase boundaries for 31 fluids generated by a well-proven comprehensive thermodynamic model. Hydrate phase boundaries for 13 independent reservoir fluids calculated by the new correlation and the thermodynamic model have been compared, showing a maximum error of 1.0 K in the calculated potential hydrate-forming temperature. The input for this correlation is the concentration of reservoir fluids in mole percent. The output of this correlation can be used to predict the base case for FPD method. The correlation has been programmed into Microsoft® Excel for ease of use. Refer *figure 4* in the next chapter for the programmed version of this correlation.

Recently, workers in Heriot-Watt University have developed two correlations to relate freezing point of water sample with hydrate formation temperature (Najibi et al., 2006). The first correlation is found to be similar to the one developed by Nielsen and Bucklin in 1983 (*Equation 2*). The second correlation is a more accurate version of the correlation which takes into account the effect of pressure. ΔT_f is the freezing point depression of the water sample, K, represents the hydrate dissociation temperature of the same fluid in the presence of distilled water, K; and P_0 represents the hydrate dissociation pressure at T_0 , bar.

$$T = T_0 - 0.6825 \times \Delta T_f \quad (3)$$

$$T = T_0 - 0.5843 \times \Delta T_f \times P_0^{0.0435} \quad (4)$$

According to Najibi and co-workers (2006), this correlation was developed based on 160 data generated using well-proven thermodynamic model. The reason of generating data using thermodynamic model instead of experimental data is due to the limited amount of experimental data available which could lead to unreliable correlation whenever an error occurred.

As a brief description of the thermodynamic model, the Valderrama modification of the Patel and Teja equation of state (VPT-EOS) has been utilized for fugacity calculations in all fluid phases while the Non-density-dependent (NDD) mixing rules are applied to model the polar-nonpolar and polar-polar interactions. The solid solution theory of van der Waals and Platteeuw is used to model the hydrate phase. The thermodynamic model also used the Kihara model for spherical molecules to calculate the potential functions for compounds forming the hydrate phase.

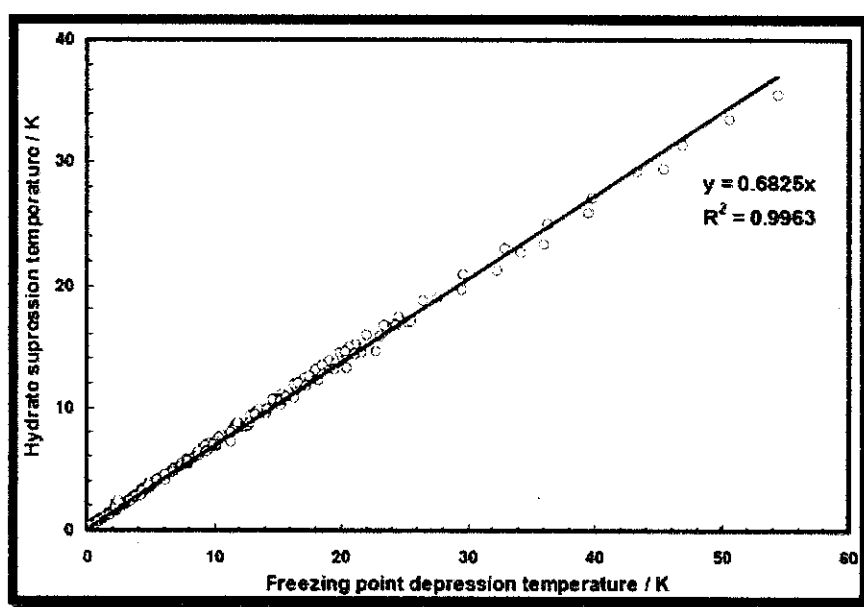


Figure 2: Hydrate suppression temperature for methane hydrates versus freezing point depression temperature in the presence of aqueous solutions containing salt and/or organic inhibitor

Figure 2 shows that the hydrate suppression is always less than the corresponding freezing point depression, which is in good agreement with the statement mentioned by Nielsen and Bucklin (1983). The inputs for both correlations are the freezing point data which could be obtain from FPD method. The hydrate dissociation temperature and pressure data could be obtain from correlation developed by Østergaard et al. (2000).

Ming Wu and co-workers has derived another correlation to relate hydrate formation temperature with inhibitor freezing point (Ming Wu et al., 2007). This equation is applicable for all inhibitors regardless of its types and concentrations. The equation is a theoretical formula for calculating the lowering of hydrate formation temperature ΔT from the lowering of inhibitor freezing point $\Delta T'$.

$$\Delta T = \frac{n\lambda'}{\lambda''} \left(\frac{T_0'}{T_0''} \right)^2 \Delta T' \quad (5)$$

Where T_0' represents the freezing point of pure water, K; λ' represents the solidification heat of pure water, K/kg; λ'' represents the solidification heat of inhibitor, K/kg; T_0'' gives the freezing point of inhibitor, K.

In this project, the correlations developed by Østergaard et al. (2000) will be used to predict the base case hydrate phase boundary for both Field A and Field B. The freezing point data generated from FPD method will be used as input to the correlations developed by Najibi et al. (2006). The usage of these reliable correlations could significantly contribute to the success of this project.

CHAPTER 3

METHODOLOGY

This project combines experimental work, correlations and simulation to accomplish its objectives. *Figure 3* provides the coordination of all the elements of study to complete this project.

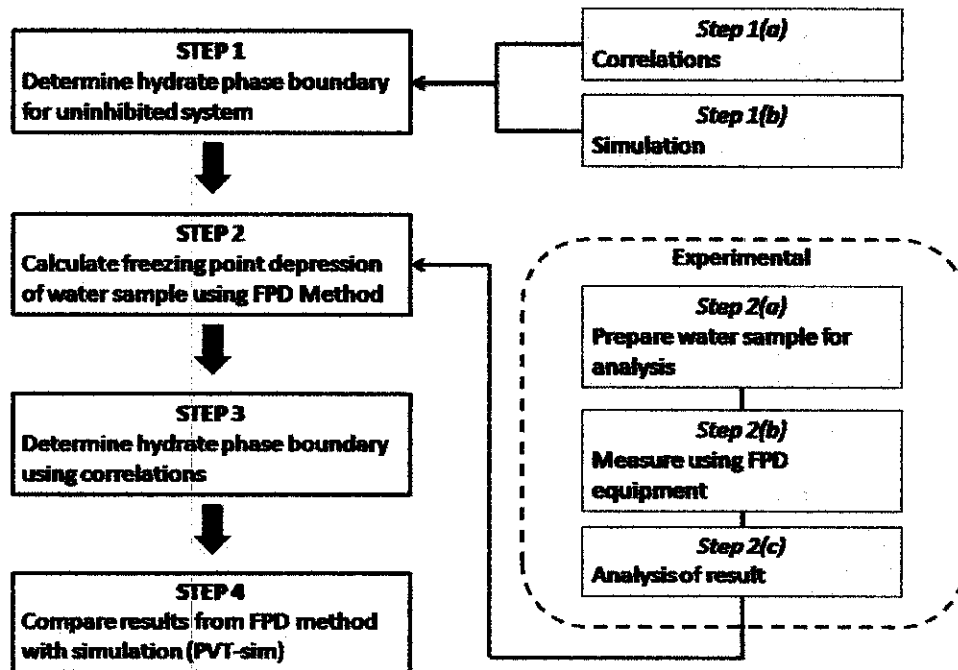


Figure 3: Step-by-step Methodology

Step 1: Developing hydrate phase boundary for uninhibited system.

Hydrate phase boundary for uninhibited system for Field A and Field B are important to this work. It acts as the base case of the study. The input needed to develop the hydrate phase boundary is the mole fraction of reservoir fluid composition. The hydrate phase boundary could be generated using a correlation or simulation. In this work, we have used correlation developed by Østergaard et al. (2000). The correlation was programmed into Microsoft® Excel for ease of use. One major assumption made was the hydrate phase boundary was calculated for reservoir fluids in the presence of distilled water.

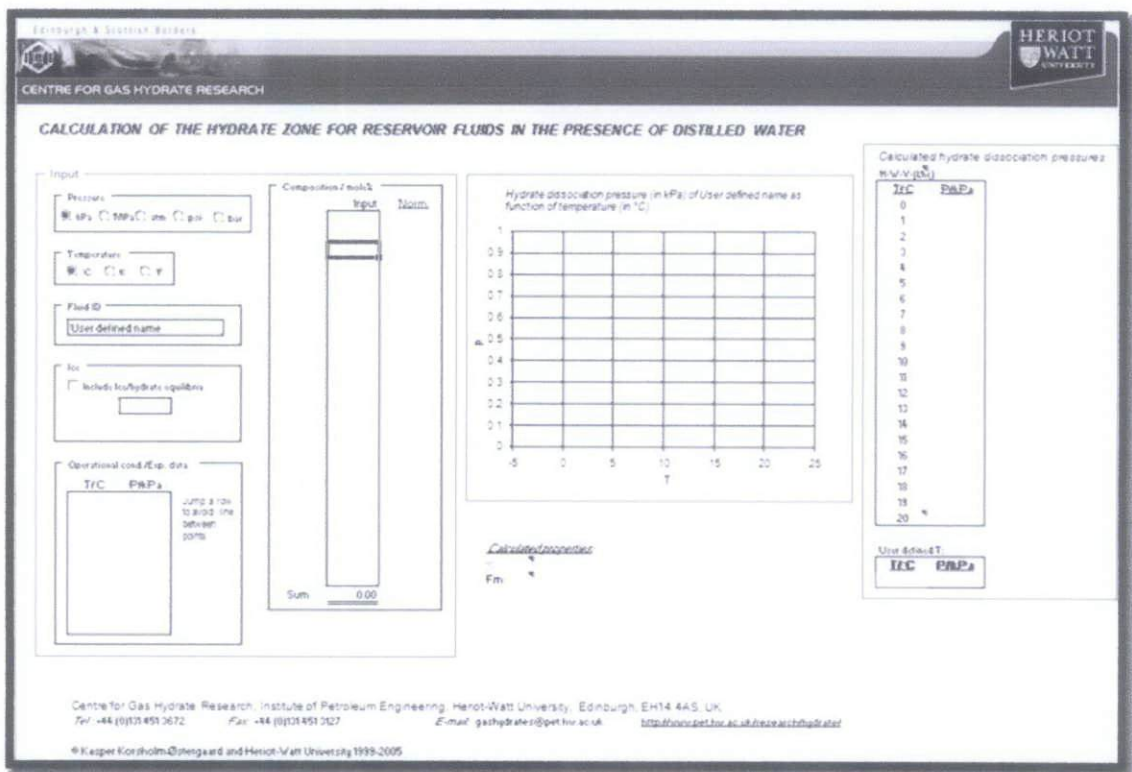


Figure 4: Correlation used to developed hydrate phase boundary with the presence of distilled water. (Source: Kasper Korsholm Østergaard and Heriot-Watt University 1999-2005)

Based on the figure above, it is clearly shown that pressure and temperature units could be manipulated accordingly. In this work, the pressure unit was set as bar and temperature unit as degrees Celsius ($^{\circ}\text{C}$). The result of using this correlation will be discussed further in **Chapter 4**. The reference and disclaimer of this correlation is attached in **Appendix A**.

Step 2: Calculating Freezing Point Depression of Aqueous Solution using Freezing Point Depression Method

Step 2(a): Preparation of water sample

Freezing Point Depression (FPD) method utilizes the feasibility of determining hydrate stability zone without the necessity of compositional analysis to the produced water sample. However in this project, we prepared a synthetic produced water sample to be analyzed using the FPD method since the real produced water sample was not available. The term ‘water sample’ used in this report refers to synthetic produced water sample of either Field A or Field B respectively. The mineral composition of each field sample is required to prepare the water sample for FPD measurement purpose. Refer **Appendix B** for the mineral composition for both fields. Based on the mineral composition, the required amount of salt was calculated. Refer **Appendix B** for the required amount of each salt to prepare water sample for Field A and Field B. The salt required was then mixed with 1 L of distilled water in a conical flask and stirred for one day.

Table 1: Salt used to prepare synthetic produced water sample

SALT	FORMULA
Calcium Chloride dihydrate	$\text{CaCl}_2 \cdot 2\text{H}_2\text{O}$
Magnesium Chloride hexahydrate	$\text{MgCl}_2 \cdot 6\text{H}_2\text{O}$
Strontium Chloride hexahydrate	$\text{SrCl}_2 \cdot 6\text{H}_2\text{O}$
Barium Chloride dihydrate	$\text{BaCl}_2 \cdot 2\text{H}_2\text{O}$
Sodium Chloride	NaCl
Sodium Sulphate	Na_2SO_4
Potassium Chloride	KCl
Sodium Carbonate	Na_2CO_3
Sodium Bicarbonate	NaHCO_3

In this work, both uninhibited and inhibited systems were tested using the FPD method. The addition of a specific amount of thermodynamic inhibitors was done to the water sample to study the effect of the inhibition. 15 wt% of Methanol and 15 wt% of Ethylene Glycol were added into the water samples in separate containers. *Table 2* below shows the entire sample prepared for analysis using FPD method in this project. The procedure for sample preparation is attached in **Appendix C**.

Table 2: Samples prepared for analysis using Freezing Point Depression method

FIELD A	FIELD B
Uninhibited	Uninhibited
Addition of 15 wt% of Methanol	Addition of 15 wt% of Methanol
Addition of 15 wt% of Ethylene Glycol	Addition of 15 wt% of Ethylene Glycol

Step 2(b): Freezing Point Depression method using prototype equipment

Theoretically, melting point and freezing point of aqueous solution has the same value at a constant pressure condition. By controlling the heating rate, the melting point of the aqueous solution could be easily measured. On the other hand freezing, in general, involves nucleation, growth and agglomeration which are time dependent processes. Thus it would be easier to measure melting point instead of freezing point. A sudden change in temperature would indicate the melting point of the solution. The analysis procedure of the freezing point, or technically melting point of water sample would be discussed in the next subsection.

The prototype equipment used in this project utilizes the rapid cooling ability of Peltier element to cool the water sample until a desired temperature. This process was done to freeze the water sample inside the sample probe. To ensure the water sample inside the sample probe is fully frozen, agitation should be done during the cooling process. Peltier element also known as Peltier cooler has some general limitations including its low efficiency and limited cooling capacity. Thus, it was

only feasible to test 1 ml of water sample each test. Then, the water sample would be heated at a specified heating rate until a certain temperature. The FPD method procedure is attached in **Appendix C**.

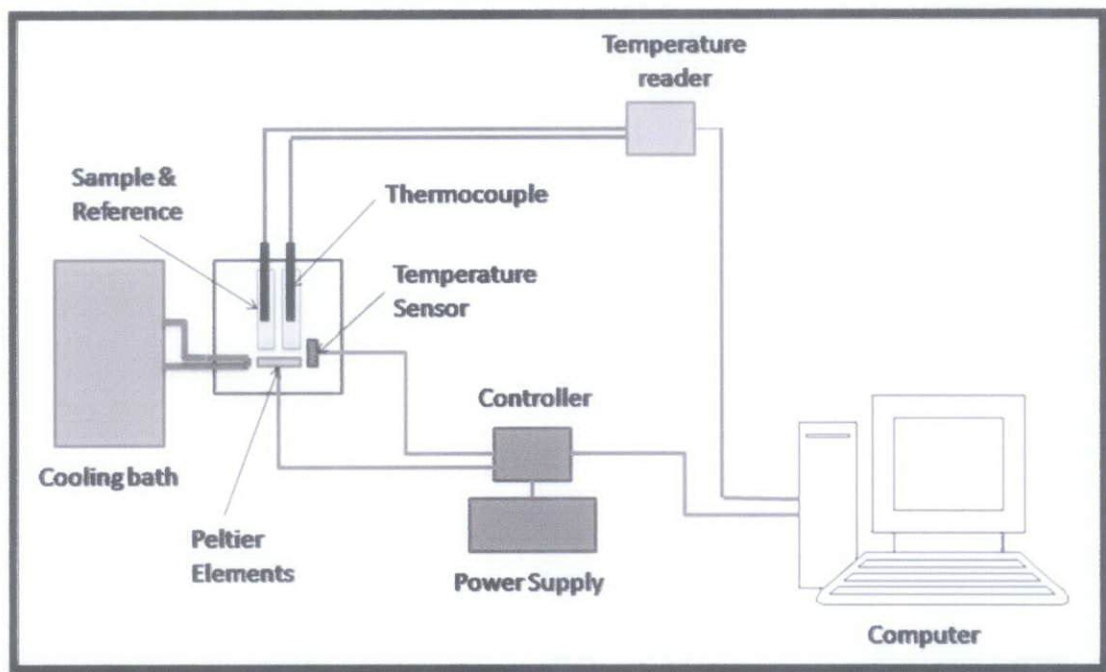


Figure 5: Schematic diagram of Freezing Point Depression prototype equipment

The figure above shows the arrangement of the major components of the prototype equipment. It should be noted that the diagram has not been illustrated according to scale. The size comparison of each component may not be accurate.

The sample and reference probe were located next to each other to minimize the temperature difference. The water sample to be tested was injected into the stainless steel sample probe while the reference probe is partially filled with thermo gel or any solution that would not freeze at low temperature. Two thermocouples of type T were inserted in both probes as a temperature reading device. Temperature reader, NI 9612 device was connected to the computer through USB interface and the thermocouples should be passed through the cap of prototype and connected to NI 9612. All temperature data would be recorded by the data acquisition software VI Logger. The cooling side of the Peltier element was located next to the sample &

reference probe. Since the heating side of the Peltier element dissipates heat as the experiments were carried out, an external cooling system was built to absorb the heat from the Peltier element. Cooling bath was used to absorb excess heat from the Peltier element. The cooling bath, set at 4 °C circulated coolant into the measurement box to remove excess heat from the heating side of the Peltier element. The measurement box holds the sample and reference probe, temperature sensor and Peltier element. It was filled with thermal insulator to minimize heat transfer between the system and the surroundings.

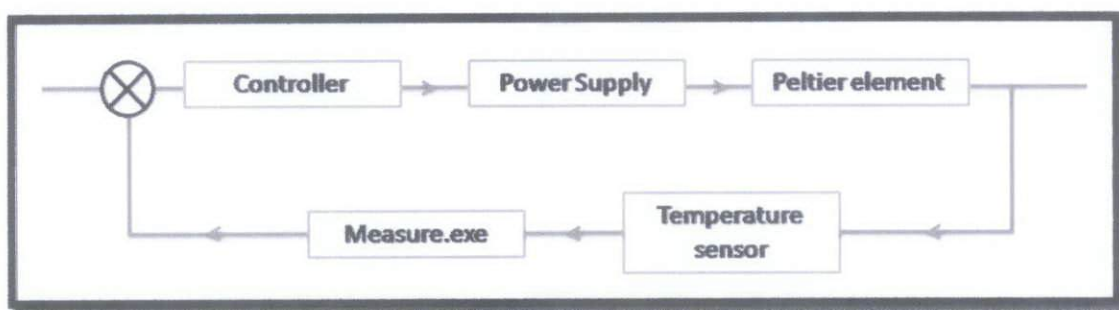


Figure 6: Temperature control system of the prototype equipment

The figure above shows the components involved in the temperature control system of the FPD prototype equipment. The temperature sensor in this prototype acts as the feedback loop which sends information to the control system software, 'Measure'. 'Measure' also provides an interface for user to input the required lowest and highest temperature in the experiment and the specific heating rate. In this project, the heating rate was specified to 0.5°C/minute. 'Measure' is responsible to send instruction to be executed by the controller. The controller controls the power supply which indirectly controls the cooling and heating mechanism of the Peltier element.

Step 2(c): Data Analysis

The temperature data recorded by the data acquisition software would be exported automatically to Microsoft® Excel for analysis. The temperature data for sample and reference would be recorded every constant interval according to the settings in the software. From the raw data exported from VI Logger, another column must be calculated which is the difference between the reference temperature and sample temperature. This process was being done to the heating region of the experiment. This data will be then plotted against the sample temperature. A peak in the plotted data would indicate a successful experiment, whereby the mixture in the sample probe was frozen. The start point of the negative slope of the peak would indicate the measured freezing point of the specific water sample. This value is then being calibrated according to the calibration value given by the manufacturer which is 0.8°C. The procedure for Data Analysis is attached in **Appendix C**.

Step 3: Determining hydrate phase boundary using correlations

This part of the project utilized the correlations developed by researchers in Heriot-Watt University (Najibi, Amir, & Tohidi, 2006). The reliability of these correlations has been discussed in **Chapter 2**.

$$T = T_0 - 0.6825 \times \Delta T_f$$

$$T = T_0 - 0.5843 \times \Delta T_f \times P_0^{0.0435}$$

The parameters required for these correlations can be obtained directly from FPD method and correlations developed by Østergaard et al. (2000). These correlations have been programmed into Microsoft® Excel to generate the data and graph. The graphical result of using these correlations is presented in **Chapter 4**.

Step 4: Comparing results from FPD method with simulation

A simulation has been completed using PVT-sim (version 17.0) for comparison purposes. The input for this simulation software is the reservoir fluid composition. The simulation software utilizes Peng-Robinson 1978 Equation of State (PR-1978 EOS) to derive the hydrate phase boundary. The limitations of this simulation software will be discussed in depth in **Chapter 4**. Using the reservoir fluid composition, the hydrate phase boundary for the uninhibited system could be developed. The inhibition effect of some common chemical could also be obtained using this simulation. Among the parameters that can be manipulated are the composition of the water sample and inhibitors composition. Due to time constraint, only one field data is simulated and compared with the results from FPD method. For this project purpose, Field B data has been used to be modeled and compared with results from FPD method. The simulation results have been presented in graphical form in **Chapter 4**. The numerical data and simulation procedure is attached in **Appendix D** and **Appendix C** respectively.

Step 5: Determine the operation pressure and temperature limits

Based on the graphical data obtained from the work done as described above, the hydrate phase boundary for uninhibited and inhibited system for deepwater operation producing 50 – 65 mol% of methane can be predicted. One major assumption has been made which is the hydrate phase boundary for reservoir fluid composed of methane ranging from 50 mol% to 65 mol% can be represented by a single curve for each inhibition effect. This assumption was made due to the observation that the differences between Field A and Field B base case curve are not significant. This assumption was also supported from the simulation results. Based on the simulation results, the inhibition effect of salt contents is getting less significant with the increase in the concentration of methanol. These observations were discussed further in **Chapter 4**.

CHAPTER 4

RESULTS AND DISCUSSION

4.1 BASE CASE SCENARIO

The base case study is an important part in this study. It provides a baseline for the FPD method experiments and the corresponding correlations.

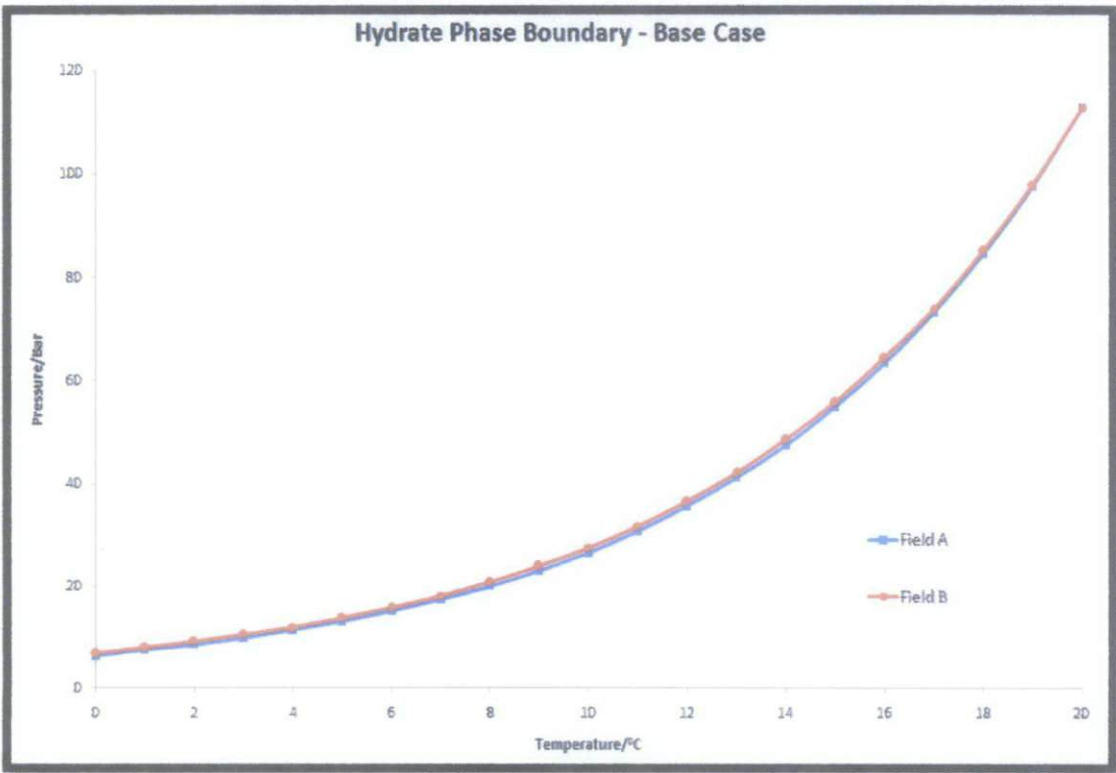


Figure 7: Base case hydrate phase boundary for Field A and Field B

The figure above shows hydrate phase boundary for Field A and Field B obtained using the correlation explained in the previous chapter. The corresponding data for each point plotted in the graph is attached in **Appendix D**. There is no

significant difference in the hydrate phase boundary curves and it is anticipated that both reservoir fluids will likely to form hydrate in the same temperature and pressure conditions. It should be noted that both reservoir fluids composed of moderate amount of methane. Based on the reservoir fluid composition data, Field A and Field B contains 52.70 mol% and 64.391 mol% of methane respectively. Thus, it is convenient to assume that fluids with methane composition ranging from 50 mol% to 65 mol% have the same hydrate phase boundary curve. It is important to note that these curves of hydrate phase boundary assume the presence of distilled water instead of produced water.

Based on this figure, it can be observed that the correlation used has limited pressure and temperature limits. The correlation is capable of developing data between 0 °C and 20 °C. In some cases, it might be necessary to have broader pressure and temperature limits.

4.2 FREEZING POINT DEPRESSION METHOD

Figure 8 shows the raw data exported from the data acquisition software to Microsoft® Excel. Based on this data, analysis was carried out to determine the freezing point of water sample for the particular test. The data analysis procedure has been described briefly in **Chapter 3** and the full procedure is attached in **Appendix C**

	A	B	C	D	E	F	G
1	NI VI Logger						
2	Created: 11/13/2007 11:02:41.793 AM Malay Peninsula Standard Time						
3	Number of scans: 13930						
4	Scan rate: 0.5 seconds						
5							
6	Row	Time	Temperatu	Temperature1(Temperature:Thermocouple)			
7	1	06:34.5	2.69846	2.7594			
8	2	06:35.0	2.70755	2.74712			
9	3	06:35.5	2.69428	2.7395			
10	4	06:36.0	2.67191	2.75105			
11	5	06:36.5	2.69108	2.73188			
12	6	06:37.0	2.68814	2.76112			
13	7	06:37.5	2.68052	2.76604			
14	8	06:38.0	2.68986	2.75768			
15	9	06:38.5	2.70165	2.74957			

Figure 8: Exported data from temperature acquisition software

The sample and reference temperatures readings were recorded using the temperature acquisition software every constant interval. In this project, the interval was set as 0.5 seconds. This interval, or scan rate can be manipulated depending on the accuracy required. It should be noted that the reducing the time interval between temperature acquisitions could result in more values recorded. This modification may increase the accuracy of the analysis but will also effect on the performance of the computer and could interrupt in the analysis of data.

Figure 9 shows the result of a single FPD test which is for Field A with 15 wt% Methanol (FA15MV1R1). This figure shows a complete result for a single test. From the figure, the measured freezing point for the particular test is -13.05°C . The results for each FPD test are attached in the Appendix section. Refer **Appendix D2** to **Appendix D7**. **Table 3** and **Table 4** show the summary of the results.

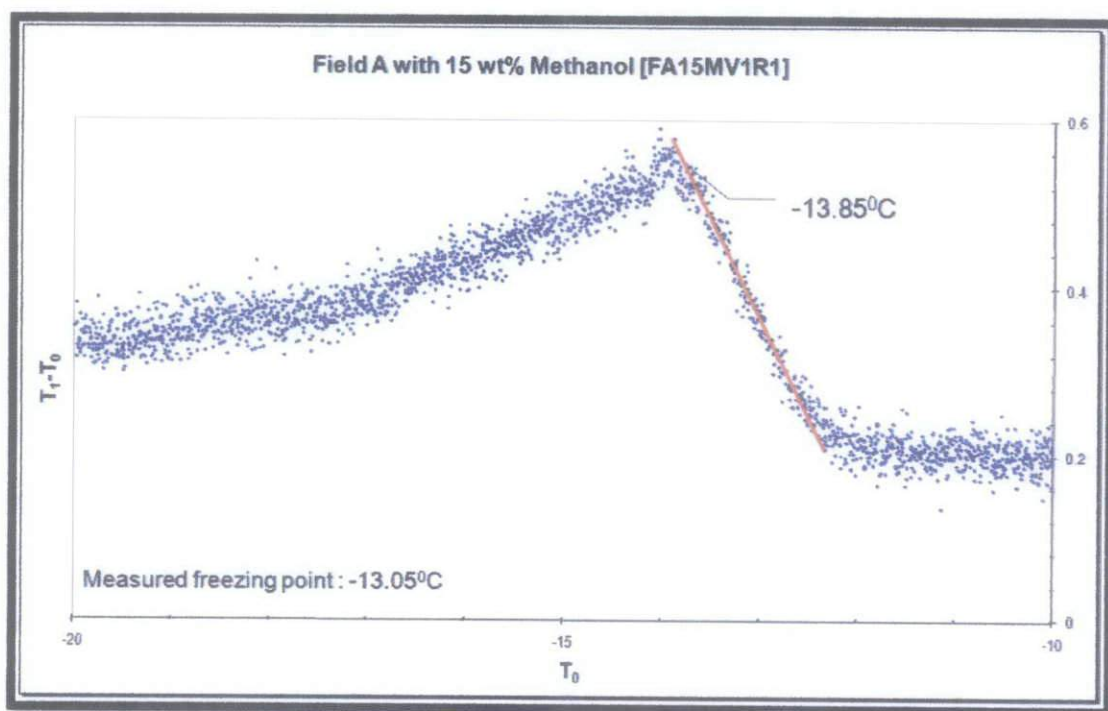


Figure 9: FPD result for Field A with 15 wt% Methanol (FA15MV1R1)

Table 3: Freezing Point Depression results for Field A

Field A		
Cooling Rate: Inf		
Heating Rate: 0.2 ⁰ C/min		
Test No	Measured Freezing Point (⁰ C)	Average (⁰ C)
Solution: Field A without Inhibition		
FAV1R1	-1.01	-0.83
FAV1R2	-0.68	
FAV1R3	-0.72	
FAV1R4	-0.92	
FAV1E1	N/A	
Solution: Field A with 15 wt% Methanol		
FA15MV1R1	-13.05	-12.78
FA15MV1R2	-13.06	
FA15MV1R3	-12.46	
FA15MV1R4	-12.86	
FA15MV1R5	-12.45	
Solution: Field A with 15 wt% Ethylene Glycol		
FA15EV1R1	-6.37	-6.71
FA15EV1R2	-6.59	
FA15EV1R3	-6.62	
FA15EV1R4	-6.85	
FA15EV1R5	-7.13	

Field B		
Cooling Rate: Inf		
Heating Rate: 0.2 ^o C/min		
Test No	Measured Freezing Point (^oC)	Average (^oC)
Solution: Field B without Inhibition		
FBV1R1	-1.24	-0.79
FBV1R2	-1.04	
FBV1R3	-0.91	
FBV1R4	-0.30	
FBV1R5	-0.45	
Solution: Field B with 15 wt% Methanol		
FB15MV1R1	-12.36	-12.09
FB15MV1R2	-12.40	
FB15MV1R3	-12.32	
FB15MV1R4	-11.80	
FB15MV1R5	-11.83	
FB15MV1R6	-11.81	
Solution: Field B with 15 wt% Ethylene Glycol		
FB15EV1R1	-7.62	-7.38
FB15EV1R2	N/A	
FB15EV1R3	-7.70	
FB15EV1R4	-6.82	
FB15EV1R5	-7.39	

Table 4: Freezing Point Depression results for Field B

Table 3 and **Table 4** show the summary of results for test done for Field A and Field B water sample respectively. Five tests were done to each solution of Field A and Field B water sample except for '*Field B with 15 wt% Methanol*' where six tests were done. Test number **FAV1E1** has encountered error during the test and the freezing point data could not be obtained. In test **FB15EV1R2**, the FPD could not be obtained since the plot of temperature difference ($T_1 - T_0$) versus sample temperature did not show any clear negative slope. This problem occurred because of the water sample in the sample container was not frozen when it was being cooled. All other tests were found to be smooth and successful.

From the tables, it can be concluded that the results have a significant degree of precision which indicates that this method is practical and suitable to be carried out for hydrate monitoring purposes. From the individual FPD data, an average value was calculated. This average FPD data for each solution were used as input to the correlations discussed in the earlier chapters. For Field A without Inhibition, an average freezing point temperature of $-0.83\text{ }^{\circ}\text{C}$ was recorded. Freezing point temperatures of $-12.78\text{ }^{\circ}\text{C}$ and $-6.71\text{ }^{\circ}\text{C}$ were recorded for Field A with 15 wt% of Methanol and Ethylene Glycol respectively. For Field B, the uninhibited system shows an average freezing point temperature of $-0.79\text{ }^{\circ}\text{C}$. For the inhibited system, freezing point temperatures of $-12.09\text{ }^{\circ}\text{C}$ and $-7.38\text{ }^{\circ}\text{C}$ were recorded for 15 wt% Methanol and Ethylene Glycol inhibition respectively.

Table 3 and **Table 4** also show the effect of methanol and ethylene glycol towards inhibiting hydrate. Although the data shown is for freezing point of water sample, similar trend is predicted when hydrate formation is taken into account. From the table, methanol has approximately twice the effect of ethylene glycol with the same mass concentration in terms of freezing point depression. Although it can be clearly shown that methanol is better than ethylene glycol, methanol tends to evaporate due to its high volatility. This effect has a great risk to the environment and also to the effectiveness of the inhibition system. Moreover, methanol is a poisonous gas and has some operational risk. The tendency of methanol to evaporate

has made this chemical is less effective in system which requires a high degree of inhibition.

The experimental works done shows that FPD method is a simple, practical and reliable method for hydrate monitoring purpose. Without the necessity for compositional analysis to the produced water sample, FPD method is easy and convenient to be carried out. The experimental works also shows a high degree of precision.

4.2.1 Limitations and Recommendations

The prototype equipment used in this project has some limitations. The main limitation is the lack of agitation mechanism. Agitation is necessary to ensure the water sample in the sample probe is fully frozen. Without the agitation mechanism, the measurement box must be agitated manually. This could lead to interruption to the connection of thermocouple and temperature sensor. It is recommended for agitation mechanism to be included in the modification of the prototype equipment.

In the prototype equipment, only one sample could be tested each time due to the existence of only one sample probe in the measurement box. The necessity of plenty of iteration requires the prototype equipment to be equipped with several sample probes. This modification would significantly decrease the experimental time of this method.

The Peltier element used in the prototype has limited cooling capability. In this project, the minimum temperature obtained is -37.5°C . Thus, the study of inhibition effect on freezing point depression of aqueous is limited to 25 wt% of Methanol and 50 wt% of Ethylene Glycol. Peltier elements with better specifications need to be identified to improve the cooling mechanism, if the application requires experimental data for higher concentrations of inhibitor.

4.2.2 Errors

The FPD method can be considered as a simple experiment. However, major errors could possibly occur during the water sample preparation process. Since the real produced water for both fields are not available, synthetic produced water sample were prepared based on the mineral composition data for each field. Although the water sample preparation process was done carefully, the sample may be exposed to contamination which could result in errors in the result obtained. Based on the calculated amount of each salt to be used in the water sample, it is impossible to weigh the exact amount of salt to be added into the distilled water. Slight difference between the required amount and the weighed amount can contribute to errors in the measurement.

Apart from this, precipitation usually occurred in the water sample during and after the preparation process due to the fact that salts have limited solubility in water. The water samples were heated and stirred during the process and before each test were carried out to minimize this type of error. This natural precipitation could lead to the error in the total amount of dissolved solids in the water composition and hence affecting the FPD results.

Slight error could also occur during the analysis of data process. Based on the procedure attached in the **Appendix C**, the freezing point value must be read manually from the start of negative slope. This type of error can be considered as human error.

4.3 CORRELATIONS

The correlations used in this project were developed by Najibi and his co-workers. Equation 3 and equation 4 were both used to obtain the hydrate phase boundary for both fields. The input to these correlations is the freezing point data obtained using the FPD method. The hydrate phase boundary developed using these correlations have been presented and discussed below.

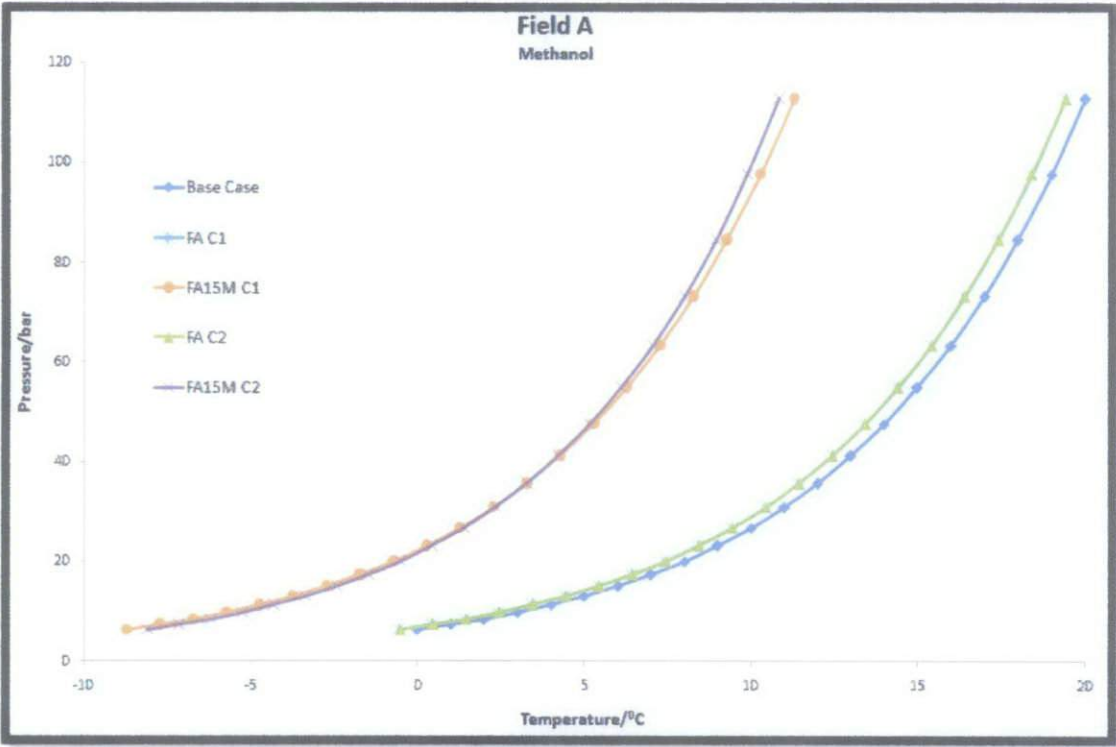


Figure 10: Prediction of hydrate phase boundary using correlation – Field A with methanol inhibition

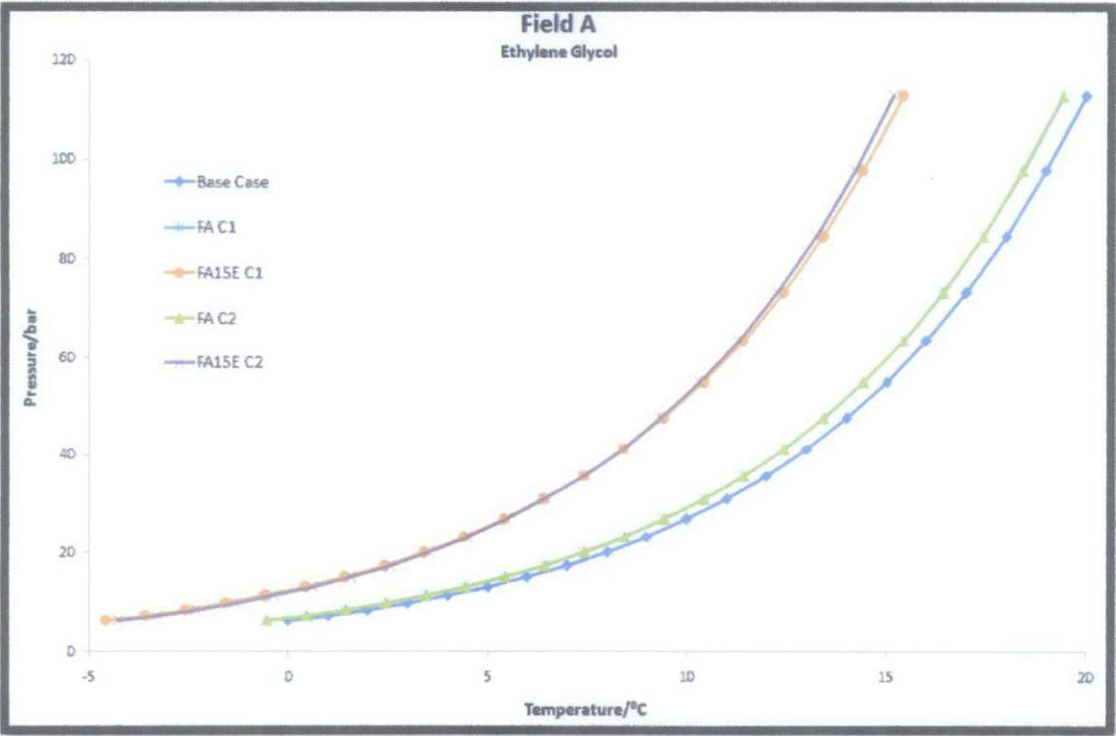


Figure 11: Prediction of hydrate phase boundary using correlation – Field A with ethylene glycol inhibition

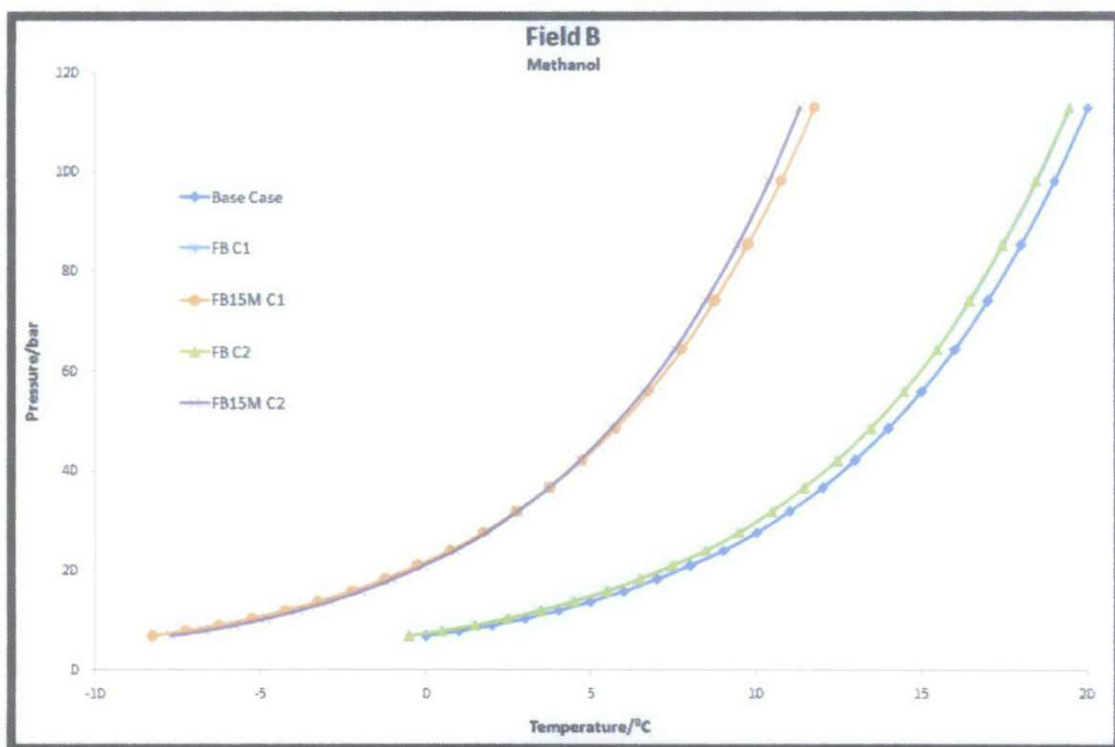


Figure 12: Prediction of hydrate phase boundary using correlation – Field B with methanol inhibition

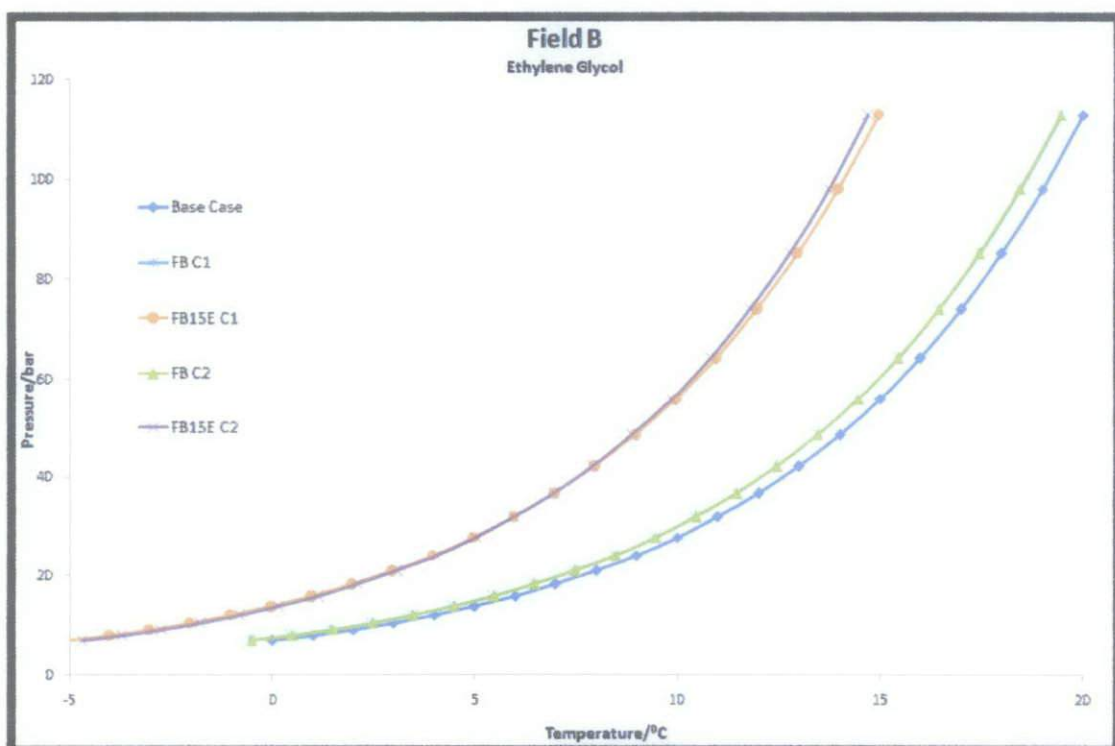


Figure 13: Prediction of hydrate phase boundary using correlation – Field B with ethylene glycol inhibition

Figure 10 to *Figure 13* show the graphical results of FPD correlated using the correlations mentioned in the previous chapter. C1 refers to equation (3) while C2 refers to equation (4). The numerical results data are attached in **Appendix D8** to **Appendix D11**.

Similar trend could be observed in all figures shown above suggesting the reliability of the FPD method and the correlations used. The lines for uninhibited field data are slightly shifted from the base case line which could be explained by the occurrence of natural inhibition due to the presence of salt in the water sample. Although the term ‘Field A without Inhibition’ and ‘Field B without Inhibition’ have been used repeatedly in this report, the natural inhibition is present due to the existence of salt in the aqueous solution. It must be clearly understood that the phrase ‘without inhibition’ in the terms stated above neglects the natural tendency of water sample to inhibit hydrate formation. In all 4 cases, the uninhibited data show good agreement between the C1 correlation and C2 correlation. For the inhibited system, all 4 cases also show good agreement between both correlations except at higher pressures. This observation is consistent with the reasons for constructing the 2nd correlation whereby it was developed to consider the effect of pressure in hydrate dissociation temperature at higher pressure conditions.

Based on the above plots, together with operation pressure and temperature data, the risk of hydrate formation in both fields could be examined. If the pressure and temperature plot intersects the hydrate phase boundary line at any point, hydrate is likely to form in that particular part of the facilities. In reality, although sufficient gas and water are available at suitable pressure and temperature conditions, time is needed for hydrate to form in the facilities. It should be noted that, this study does not take into account the kinetics of hydrate formation which include nucleation, growth and formation. The kinetics of hydrate formation is time dependent parameters. Thus, any slight intercepts would not be favorable for this study although the intercepts only takes place for a short time.

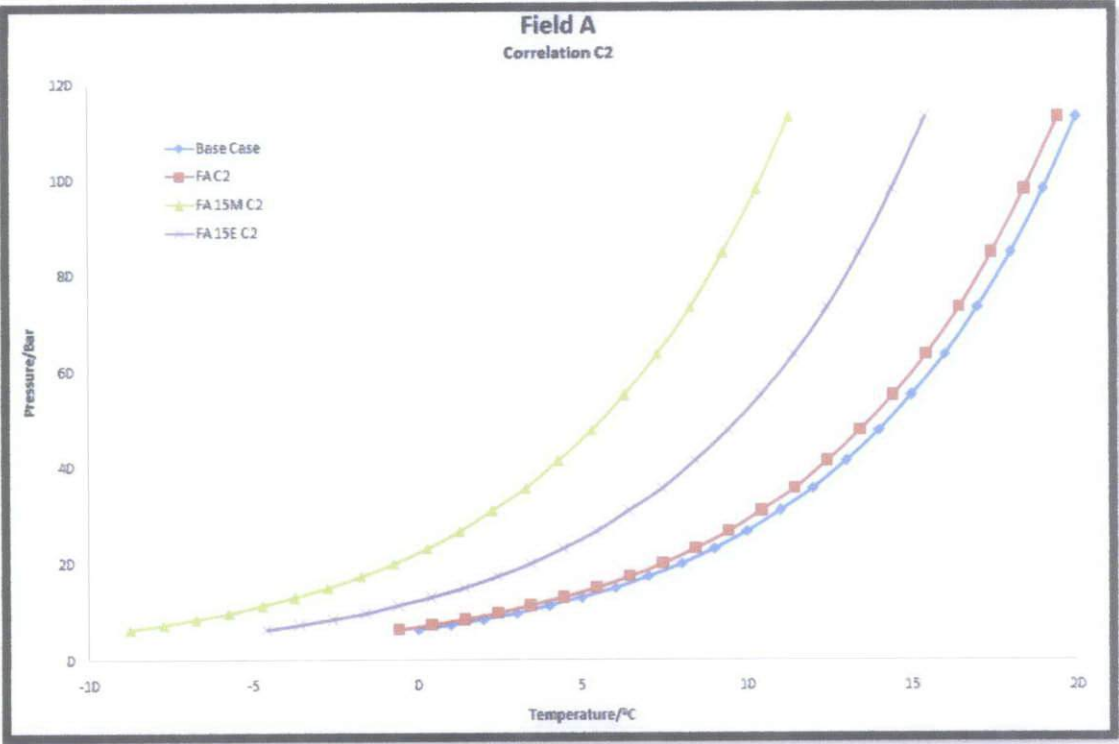


Figure 14: Comparison of Methanol and Ethylene Glycol towards shifting hydrate phase boundary for Field A

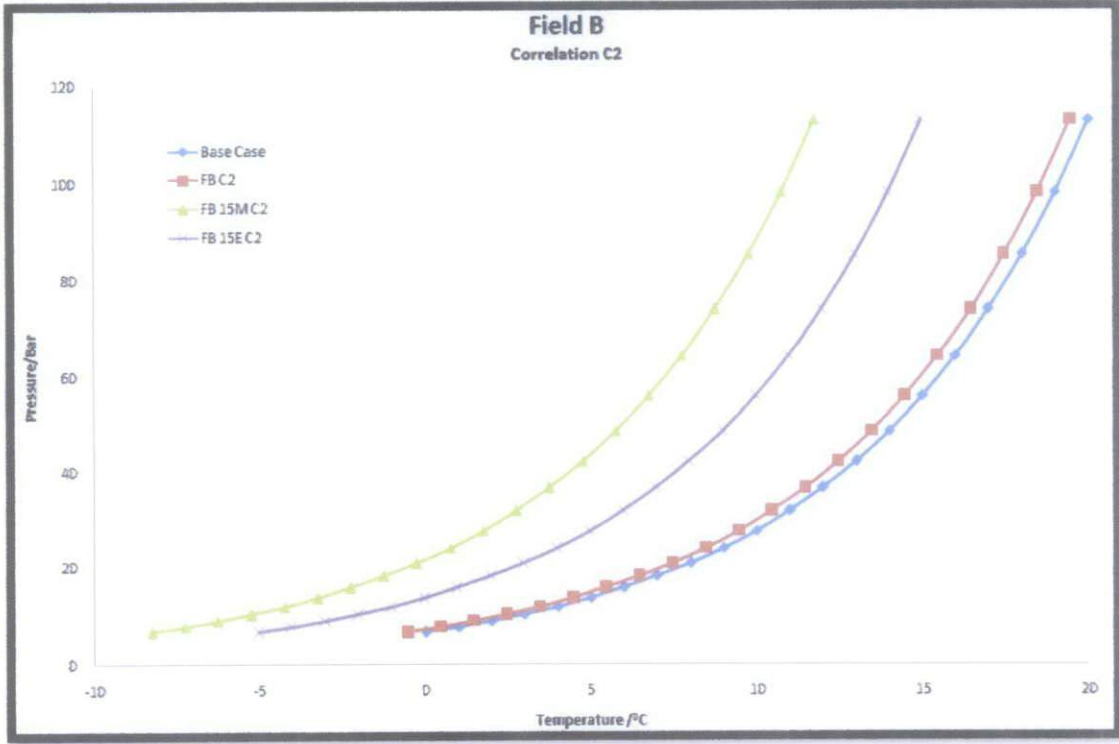


Figure 15: Comparison of Methanol and Ethylene Glycol towards shifting hydrate phase boundary for Field B

4.4 SIMULATION

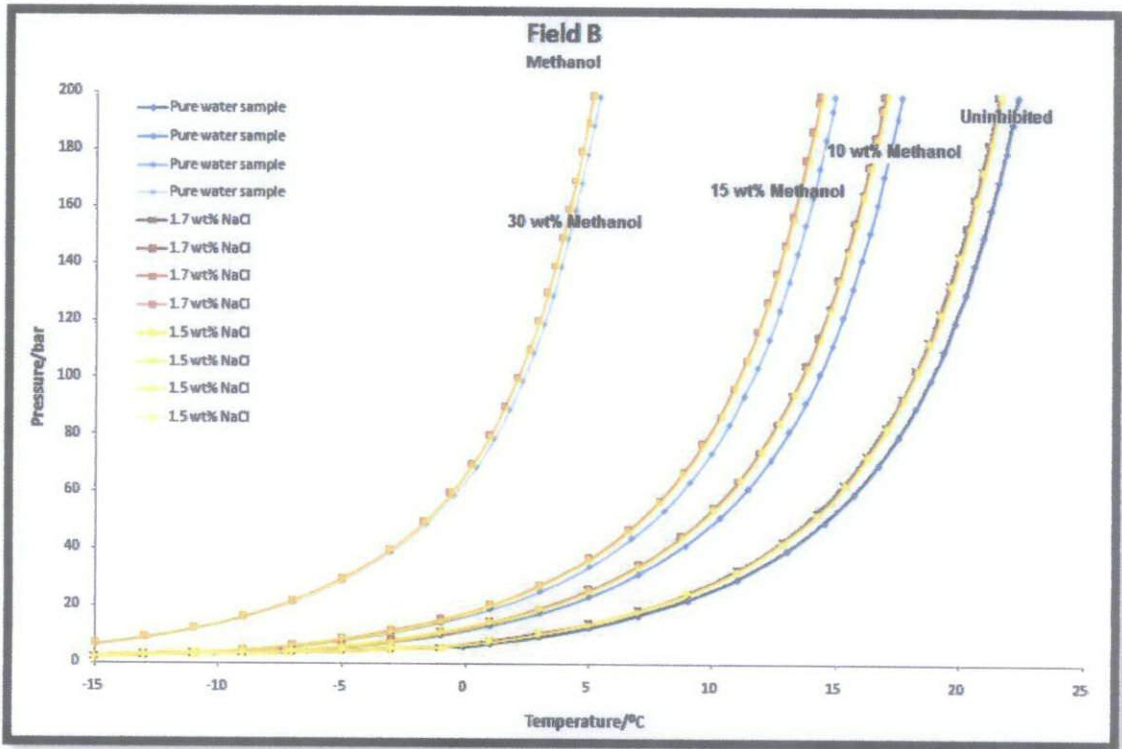


Figure 16: Graphical results of simulation using PVT-sim

The figure above shows the simulation results obtained using PVT-sim. The blue colored lines in the figure represent the simulation of pure water sample which has no natural inhibition at all. The red lines represent water sample of 1.7 wt% NaCl and the yellow represent water sample of 1.5 wt % NaCl. The simulation is not capable of modeling the exact composition of produced water sample. Based on the mineral composition of Field B water sample (**Appendix B**), only sodium (Na), potassium (K), chloride (Cl), sulphate (SO₄), and bicarbonate (HCO₃) are assumed to be significant to naturally inhibit hydrate formation. To overcome the limitations of the simulation software, these mineral contents have been assumed to be represented by sodium and chloride only. For 1.7 wt% NaCl, all the minerals stated above are considered while for 1.5 wt% NaCl, sulphate contents are neglected.

The simulation was done 4 times for each water sample to study the result of uninhibited system and inhibited system with different thermodynamic inhibitors

concentration. 3 different concentrations of thermodynamic inhibitors chosen for this study are 10 wt% Methanol, 15 wt% Methanol and 30 wt% Methanol.

Based on the figure above, the spacing between different inhibitor concentrations can be considered as consistent. It can be observed that the natural inhibition of water sample towards hydrate formation is getting less significant with the increase of methanol concentration. This observation is a critical towards developing an assumption for the outcome of the project which is discussed in **Section 4.5**

Compared to the results obtained from FPD method, the simulation software has wider pressure and temperature limits. This is probably the main advantage of the simulation software compared to the FPD method. In addition to this, the simulation software would also be able to simulate various composition of inhibitor in a short time.

Comparison has been made between results obtained from FPD method with results from PVT-sim. Based on the figure below, the simulation result has shown some degree of similarity with the results obtained from FPD method. This shows that the results obtained from FPD method is reliable. In the uninhibited system, the plot of simulation result is very close to the existing plot. Some significant difference in the inhibited system can be observed between FPD method result and simulation result. This difference may occur due to the limitations or major assumptions of the simulation software. Despite these differences, the simulation results have shown that the FPD method is a reliable method for hydrate monitoring.

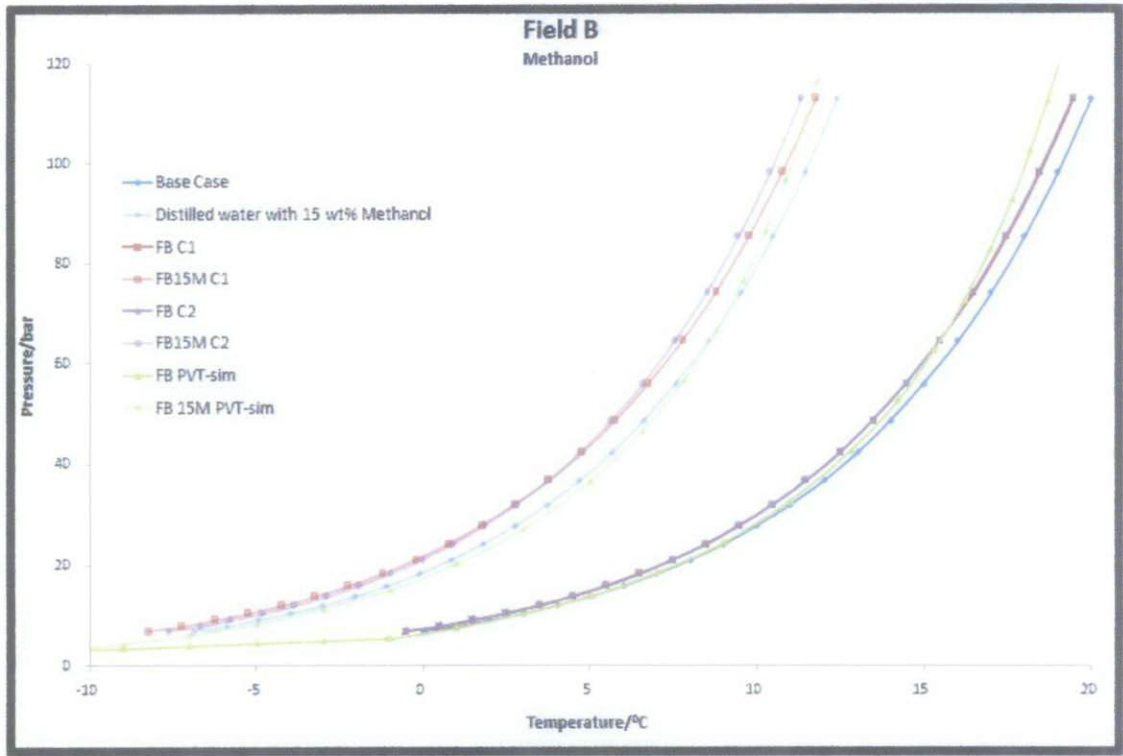


Figure 17: Graphical comparisons between results from FPD method and PVT-sim

As explained in the earlier part of this chapter, the FPD prototype equipment used in this project has limited capabilities which can be overcome using PVT-sim. For higher degree of inhibition effect, simulation using PVT-sim could be done to obtain required data. However, it should be noted that the simulation software has less accuracy compared to the FPD method which suggests the necessity of higher safety factor to be used in the hydrate monitoring strategy.

4.5 SUITABLE OPERATION CONDITIONS

Based on the work done, it is possible to determine the operation temperature and pressure limits for deepwater fields producing moderate amount of methane. In this project, moderate amount refers to the range of 50 mol% to 65 mol% methane in the reservoir fluid. Equation (4) or C2 correlation was used to develop the hydrate phase boundary curves for inhibited and uninhibited system. Equation (4) was selected instead of Equation (3) because of the latter equation neglects the effect of pressure in higher pressure conditions.

It is assumed that different reservoir fluids with methane composition within the specified range have the same hydrate phase boundary curve. This major assumption was made due to the fact that there is not much difference between hydrate phase boundary curves for Field A and Field B which compose of 52.70 mol% and 64.391 mol% methane respectively. This observation was made to the base case scenario results in **Section 4.1**. This assumption also considers methane as the main hydrate former in natural gas. With a significant composition of methane in the reservoir fluid, the composition of methane has been seen as the key factor in the hydrate phase boundary. The simulation results shown in *Figure 16* had proved that the natural inhibition of salt content in the produced water is less significant at high thermodynamic inhibitor content. In other words, the natural inhibition of salt is not the critical factor in determination of hydrate phase boundary.

Based on the assumption described above, separate curves from Field A and Field B can be merged into a single curve. Each point on the curves has its numerical value. Values for Field A and Field B are averaged to obtain a new curve representing hydrate phase boundary for reservoir fluid composed of moderate amount of methane. The figure below shows the outcome of this project which is the graphical representation of operation pressure and temperature limits for reservoir producing 50 – 65 mol% of methane.

Figure 18 shows the overall outcome of this project in a graphical form. There are 4 different curves plotted in the figure which are for the base case, uninhibited system, 15 wt% of ethylene glycol inhibition and 15wt% of methanol inhibition. It should be noted that the difference between base case and uninhibited system is the latter includes the natural inhibition of salt content in the produced water. The base case assumes the presence of distilled water. Based on this figure, the suitable working pressure and temperature for deepwater operation producing 50 – 65 mol% of methane can be predicted. Without any inhibition, the operation is highly exposed to the risk of hydrate formation.

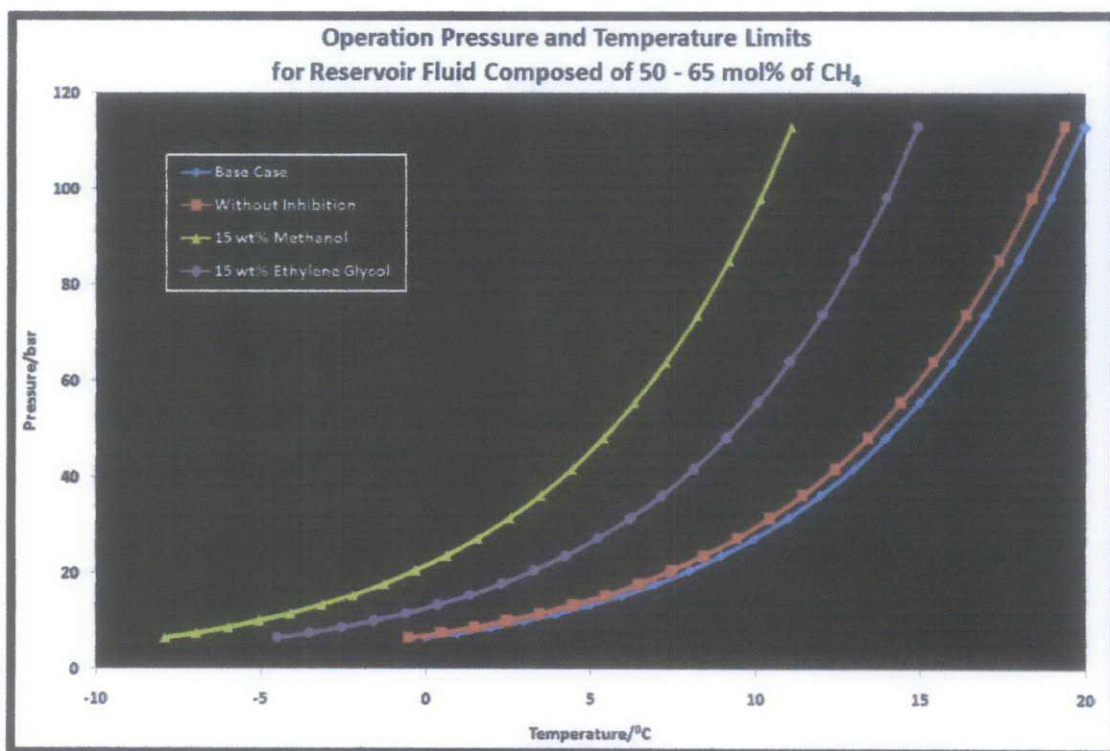


Figure 18: Graphical representation of operation pressure and temperature limits for reservoir producing 50 - 65 mol% of methane

Figure 18 also shows the inhibition effect of 15 wt% ethylene glycol and 15 wt% of methanol. At 15 wt%, it is observed that methanol has better performance compared to ethylene glycol towards shifting hydrate phase boundary. Various publications have made the comparisons between methanol and ethylene glycol towards shifting hydrate phase boundary. The outcome of this project has proven that methanol has better capability of shifting of hydrate phase boundary. However, this project only shows the result of test done with 15 wt% of both inhibitors and may not be used to predict the hydrate phase boundary curve for higher concentrations of inhibitors.

It should be noted that the outcome of this project shown in *Figure 18* is an empirical approach. The reliability of the outcome depends on the experimental procedure and correlations used in accordance with FPD method. Although the experiments have been done carefully, error may still occur throughout the projects. It is recommended to shift the curves 1 – 2 °C to the right. This can be considered as

an analogy to safety factor used in engineering calculations. By shifting the curves to the right, any system would be likely to be exposed to a higher risk of hydrate formation. This would give a safety margin to the particular system.

Figure 18 can be used as a guideline for the use of thermodynamic inhibitors (methanol and ethylene glycol) in shifting hydrate phase boundary both in the industry or for academic purposes. However, it is meant only for reservoir producing moderate amount of methane which is defined in this project as 50 – 65 mol%. Any interception of the operation pressure and temperature curves can be an early indication of the risk of hydrate formation in the particular area.

Part of this project can be extended further to find the curves for other ranges of methane composition in the reservoir fluid. Besides that, it might be necessary to include other concentrations of methanol and ethylene glycol. Based on the limitations and recommendations discussed in **Section 4.2.1**, improvement on the prototype equipment can be initiated as an extension to this project.

CHAPTER 5

CONCLUSION

This project is significant to the oil and gas industry especially to companies focusing on deepwater exploration and production. The results of this study can be used as a guideline for implementing Freezing Point Depression method for hydrate monitoring. With the operation pressure and temperature data, the risk of hydrate formation in reservoir producing moderate amount of methane could be studied, giving a clear idea on the actions to be taken as part of the flow assurance strategy. The project shows that hydrate monitoring strategy could be simplified significantly using water sampling. The tests done for water sample from Field A and Field B have shown a precise data using the Freezing Point Depression prototype equipment. The limitations of the prototype equipment have been discussed at length for future modification process. The FPD data were used as input to the correlations developed by researchers to obtain hydrate phase boundary. With the hydrate phase boundary, the prediction of hydrate formation temperature and pressure conditions could be done. The graphical result obtained shows that the reliability of the correlations used. Based on the comparison made between results obtained from FPD method and PVT-sim, it is justified that the experiment results and correlations used in accordance with FPD method are reliable. The objectives of this project have been achieved where the FPD method has been successfully carried out to obtain a graphical representation of hydrate phase boundary for reservoir producing moderate amount of methane. The inhibition effect of two common inhibitors used in the industry has also been discussed.

REFERENCES

- Chatti, I., Delahaye, A., Fournaison, L., Petitet, J-P. (2005). Benefits and Drawbacks of Clathrate Hydrates: A Review of their Areas of Interest, *Energy Conversion and Management*, 46, 1333-1343.
- Hammerschmidt, E.G. (1939) Gas Hydrate Formation, A Further Study On Their Prevention and Elimination from Natural Gas Pipe Lines, *Gas*, 15 (5), 30-34.
- Mohammadi, A.H., Martínez-López, J.F. and Richon, D. (2007). Determination of Hydrate Stability Zone Using Electrical Conductivity Data of Salt Aqueous Solution, *Fluid Phase Equilibria*, 253, 36-41.
- Mohammadi, A.H., Martínez-López, J.F. and Richon, D. (2007). Predicting Hydrate Stability Zones of Petroleum Fluids Using Sound Velocity Data of Salt Aqueous Solutions, *Fluid Phase Equilibria*, 253, 165-170.
- Najibi, H., Mohammadi A.H. and Tohidi, B., (2006). Estimating the Hydrate Safety Margin in the Presence of Salt and/or Organic Inhibitor using Freezing Point Depression Data of Aqueous Solution, *Ind. Eng. Chem. Res.*, 45, 4441-4446.
- Nielsen, R.B. and Bucklin, R.W. (1983). Why not use methanol for hydrate control?, *Hydrocarbon Process*, 62 (4), 71-78.
- Østergaard, K.K., Tohidi, B., Danesh, A., Todd A.C., and Burgass R.W. (2000). A General Correlation for Predicting Hydrate-Free Zone of Reservoir Fluids, *SPE Production and Facilities*, 15(4), 228-233.
- Sloan, E.D. (1998). Clathrate Hydrates of Natural Gases (2nd ed.). New York: Marcel Dekker.
- Wu, M., Wang, S., Liu, H. (2007). A Study on Inhibitors for the Prevention of Hydrate Formation in Gas Transmission Pipeline, *Journal of Natural Gas Chemistry*, 16, 81-85.

APPENDICES

APPENDIX A	REFERENCE AND DISCLAIMER
APPENDIX B	FIELD DATA
APPENDIX C	PROCEDURES
APPENDIX D	RESULTS

APPENDIX A

REFERENCE AND DISCLAIMER

© Kasper Korsholm Østergaard and Heriot-Watt University 1999-2005

References:

- 1) Østergaard, K.K., Tohidi, B., Danesh, A., Todd, A.C., and Burgass, R.W.: "A General Correlation for Predicting the Hydrate-Free Zone of reservoir Fluids", SPE Production & Facilities, Vol. 15(4), 228-233 (2000).
- 2) Østergaard, K.K., and Tohidi, B.: "A Correlation for Predicting the Hydrate Stability Zone in the Presence of Ice", Proceedings of the 4th International Conference on Gas Hydrates", Yokohama, 19-23 May, 384-387 (2002).

Disclaimer:

Although this software has been tested with care, it is not guaranteed for any purpose. It is not designed, manufactured or intended for use in any situation in which the failure of this software could lead directly to death, personal injury, physical or environmental damage, or financial loss. The authors do not accept liability for any loss, costs, damages or expenses sustained by anyone resulting from the use of this software.

APPENDIX B

FIELD DATA

Table B1: Mineral Composition Data for Field A and Field B water sample

	Field A (mg/L)	Field B (mg/L)
Sodium	5360	6980
Potassium	46	1200
Calcium	150	91
Magnesium	19	23
Barium	4	Nil
Strontium	2.4	5.2
Total Iron	Nil	35
Chloride	7350	10000
Sulphate	73	1390
Bicarbonate	2530	1870
Carbonate	Nil	Nil
Hydroxide	Nil	Nil
Total dissolved solids	15540	21570
Total suspended solids	Nil	1028

Table B2: Reservoir Fluid Composition for Field A (Simplified Version)

Component	Mole Percent
N ₂	0.05
C0 ₂	0.44
C1	52.70
C2	5.73
C3	4.39
iC4	0.82
nC4	1.74
iC5	0.78
nC5	0.79
C6	3.11
C7	3.70
C8	3.11
C9	1.73
C10	1.71
C11	2.09
C12	2.05
C13	2.03
C14	2.01
C15	2.03
C16	1.36
C17	1.11
C18	1.18
C19	0.86
C20	4.48

Table B3: Reservoir Fluid Composition for Field B (Simplified Version)

Component	Mole Percent
N ₂	0.241
CO ₂	0.19
C1	64.391
C2	3.959
C3	3.137
iC4	0.722
nC4	1.774
iC5	0.762
nC5	0.912
C6	1.323
m-c-C5	0.48
Benzene	0.13
c-C6	0.46
m-c-C6	0.72
Toluene	0.29
et-Benzene	0.15
p-Xylene	0.27
o-Xylene	0.14
Ps-Cumene	0.14
C7	1.215
C8	1.455
C9	1.274
C10-C12	3.698
C13-C15	3.027
C16-C18	2.245
C19-C23	1.956
C24-C29	1.446
C30-C36	1.184
C37-C45	0.987
C46-C57	0.747
C58-C80	0.576

Table B4: Required salt to prepare synthetic produced water sample for Field A

Salt	Formula	Field A (g)
Calcium Chloride dihydrate	$\text{CaCl}_2 \cdot 2\text{H}_2\text{O}$	0.5502246
Magnesium Chloride hexahydrate	$\text{MgCl}_2 \cdot 6\text{H}_2\text{O}$	0.1589588
Strontium Chloride hexahydrate	$\text{SrCl}_2 \cdot 6\text{H}_2\text{O}$	0.007303
Barium Chloride dihydrate	$\text{BaCl}_2 \cdot 2\text{H}_2\text{O}$	0.0071136
Sodium Chloride	NaCl	11.028795
Sodium Sulphate	Na_2SO_4	0.1079792
Potassium Chloride	KCl	0.0877059
Sodium Carbonate	Na_2CO_3	0
Sodium Bicarbonate	NaHCO_3	3.4839344
Total salt (g)		15.432014
Total dissolved solids from sum of ions (mg)		15534.4

Table B5: Required salt to prepare synthetic produced water sample for Field B

Salt	Formula	Field B (g)
Calcium Chloride dihydrate	$\text{CaCl}_2 \cdot 2\text{H}_2\text{O}$	0.333803
Magnesium Chloride hexahydrate	$\text{MgCl}_2 \cdot 6\text{H}_2\text{O}$	0.192424
Strontium Chloride hexahydrate	$\text{SrCl}_2 \cdot 6\text{H}_2\text{O}$	0.015823
Barium Chloride dihydrate	$\text{BaCl}_2 \cdot 2\text{H}_2\text{O}$	0
Sodium Chloride	NaCl	12.57199
Sodium Sulphate	Na_2SO_4	2.056042
Potassium Chloride	KCl	2.28798
Sodium Carbonate	Na_2CO_3	0
Sodium Bicarbonate	NaHCO_3	2.575082
Total salt (g)		20.03315
Total dissolved solids from sum of ions (mg)		21559.2

APPENDIX C

PROCEDURES

Sample Preparation

Preparing synthetic produced water from Field A and B.

1. Calculate the amount of salt need to be used to represent the water sample from Field A and Field B.
2. Prepare and weigh each salt according to the calculation done earlier.
3. Add each salt into a 1 L conical flask partially filled with distilled water and stir for 5 minutes after adding each salt.
4. Fill the conical flask with distilled water until reaching the 1 L mark.
5. Stir the mixture for overnight to assure all the salt has dissolved in the distilled water.
6. Label each conical flask with “Field A” and “Field B” respectively.

Addition of Thermodynamic Inhibitors

1. By using an electronic scale, weigh an empty 50ml conical flask. Re-zero the scale and wait until it stabilizes.
2. Carefully add in water sample into the conical flask and wait until the reading of the electronic scale stabilizes.
3. From the reading, calculate the amount of thermodynamic inhibitors needs to be injected into the water sample to obtain the desired inhibition.

$$y = \frac{m_I}{(100 - m_I)} x$$

$$v = \frac{y}{\rho_I}$$

Where x = mass of water sample (from the electronic scale reading)

y = required mass of thermodynamic inhibitor

m_I = desired mass percent of thermodynamic inhibitor

ρ_I = density of thermodynamic inhibitor

v = required volume of thermodynamic inhibitor

	A	B	C	D	E	F	G
1	NI VI Logger						
2	Created: 11/13/2007 11:02:41.793 AM Malay Peninsula Standard Time						
3	Number of scans: 13930						
4	Scan rate: 0.5 seconds						
5							
6	Row	Time	Temperatu	Temperature1(Temperature:Thermocouple)			
7	1	06:34.5	2.69846	2.7594			
8	2	06:35.0	2.70755	2.74712			
9	3	06:35.5	2.69428	2.7395			
10	4	06:36.0	2.67191	2.75105			
11	5	06:36.5	2.69108	2.73188			
12	6	06:37.0	2.68814	2.76112			
13	7	06:37.5	2.68052	2.76604			
14	8	06:38.0	2.68986	2.75768			
15	9	06:38.5	2.70165	2.74957			

Figure C1: Exported Temperature Data

Data Analysis

1. In MS Excel, the exported data needs to be manually analyzed (Refer figure C2 – C4).
2. Calculate additional column: Reference temperature (T_1) – Sample Temperature (T_0).

Note: This process is being done the heating region of the system only.

3. Plot difference between reference and sample temperature against sample temperature ($T_1 - T_0$ versus T_0) in the heating region.
4. In the constructed plot, find the start of the declining slope which indicates the freezing point temperature.
5. As a final stage, add 0.8°C to the value from step 4 to obtain the calibrated measured freezing point of the sample.

	A	B	C	D	E	F	G	H
1	T0	T1	T1-T0					
2	-25.234	-25.023	0.211					
3	-25.2413	-24.9992	0.2421					
4	-25.2371	-25.034	0.2031					
5	-25.2356	-25.0322	0.2034					
6	-25.2101	-25.0154	0.1947					
7	-25.2474	-24.9997	0.2477					
8	-25.2075	-24.995	0.2125					
9	-25.2311	-24.9827	0.2484					
10	-25.2057	-24.9887	0.217					
11	-25.2025	-24.9811	0.2214					
12	-25.1965	-24.9911	0.2054					
13	-25.2101	-24.9607	0.2494					
14	-25.1721	-24.9722	0.1999					
15	-25.1695	-24.9452	0.2243					

Figure C2: Calculate additional column, reference temperature (T_1) – sample temperature (T_0)

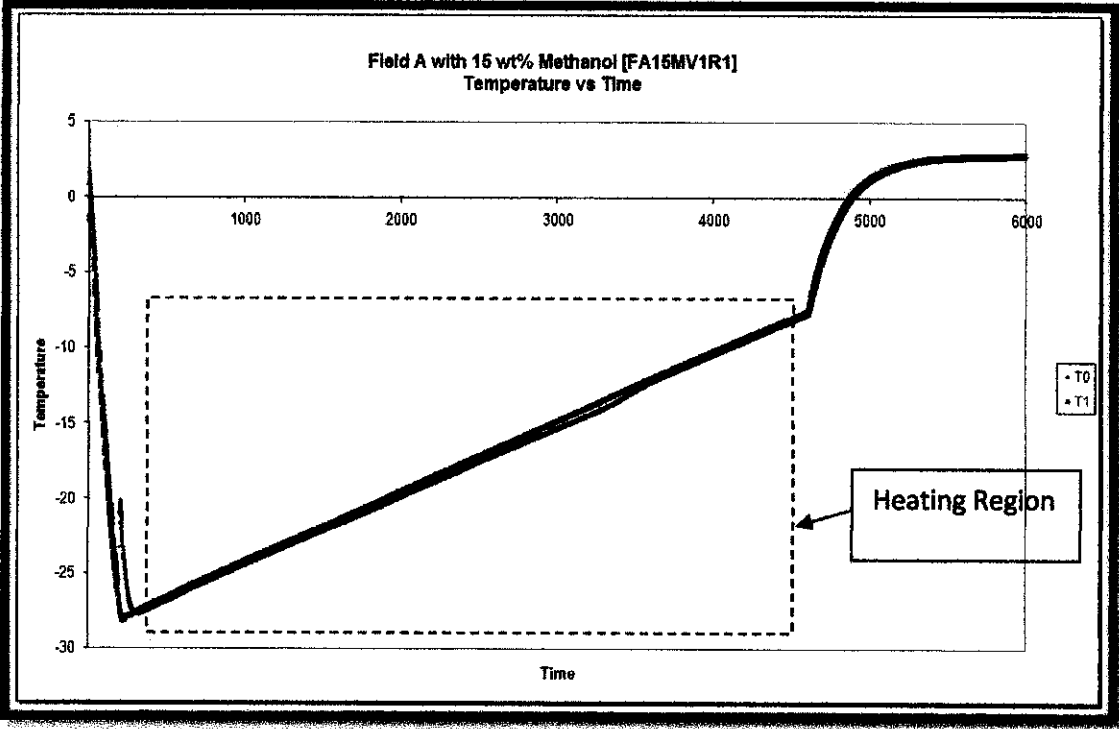


Figure C3: Heating region of the system

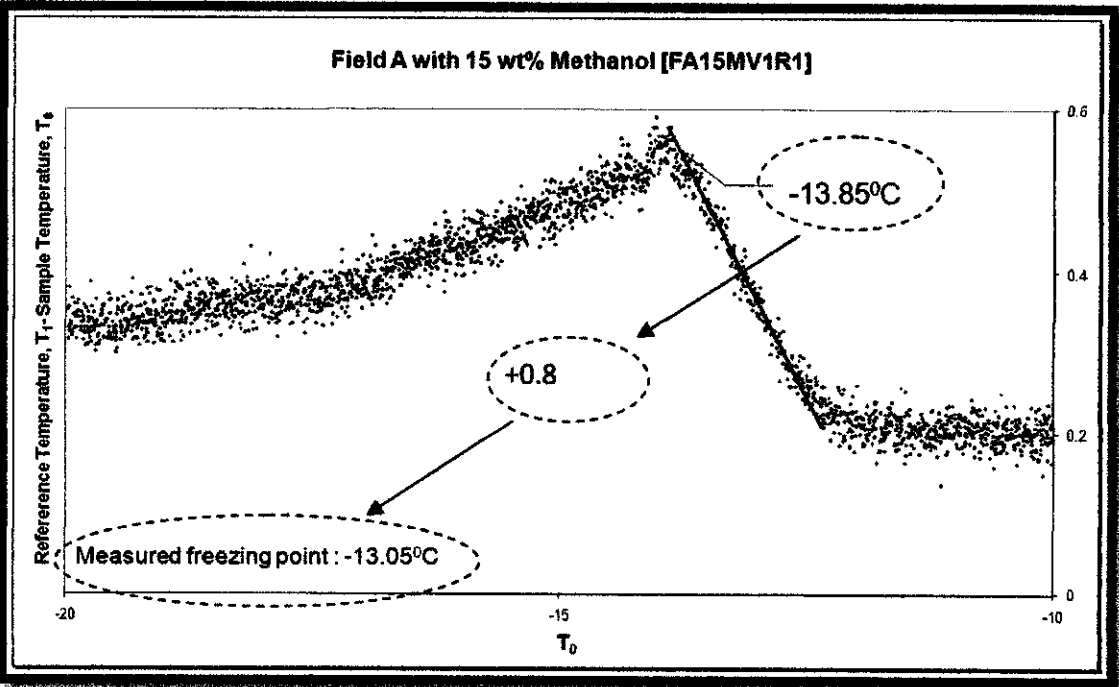


Figure C4: Difference between reference and sample temperature versus sample temperature

Simulation Procedure

1. Open PVT-sim (version 17.0).

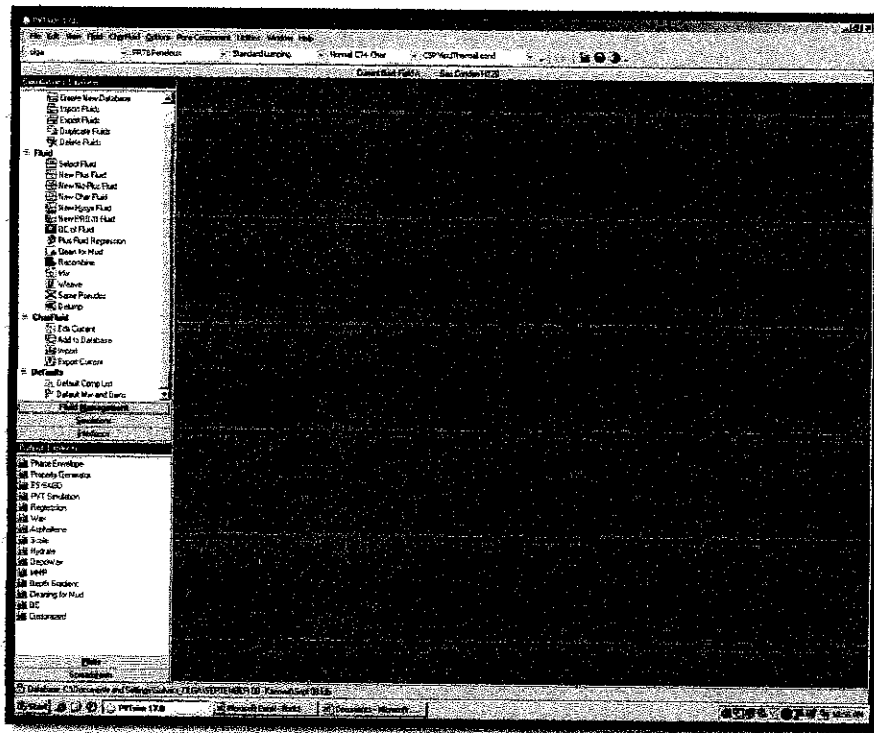


Figure C5: User Interface for PVT-sim (ver 17.0)

2. Click on **Fluid Management**.
3. If the reservoir fluid is not in the database, new fluid data must be added to the database.
4. Select **New Plus Fluid**. A dialog box will appear.

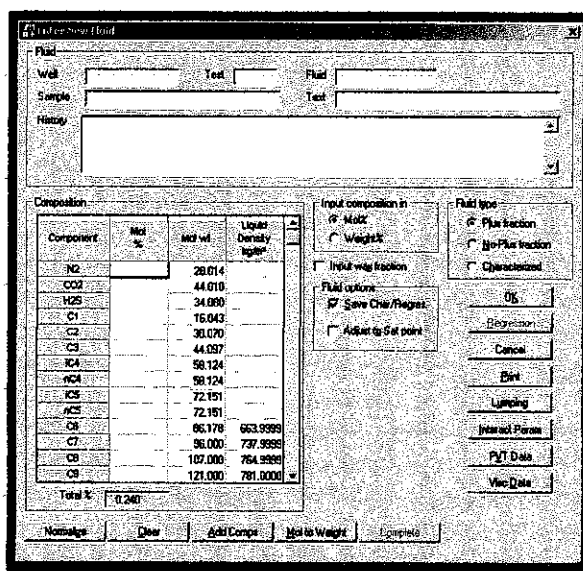


Figure C6: Dialog box for new fluid composition

5. Fill in the reservoir fluid composition in the required box. Fill in either field name, well name or sample name in the respective box for fluid identification purpose.
6. If the fluid is not in the list, select **Add Comps.** Components can be added into the list.

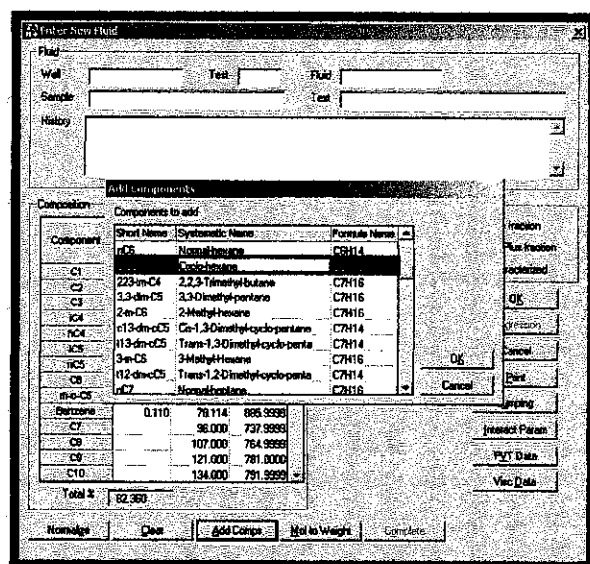


Figure C7: Components can be added into the list

7. Click **OK**. The reservoir fluid is now in the database.
8. To start simulation, click on **Simulation**.

9. Select **Hydrate** from the **Flow Assurance** list.

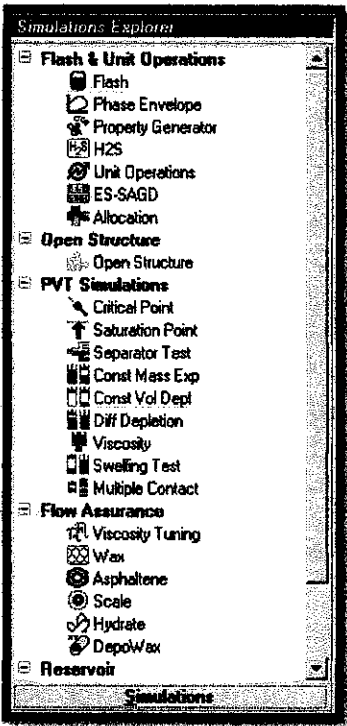


Figure C8: Various options in the Simulation Explorer

10. In the **Water Specification** section, fill in any value in the **Amount** field and select %water cut. Fill in the desired value in the **Composition** field.
11. In the **Inhibitor Specification** section, fill in the desired value in the **Amount** field and **Composition** field respectively.
12. Click **Hydrate PT Curve**.

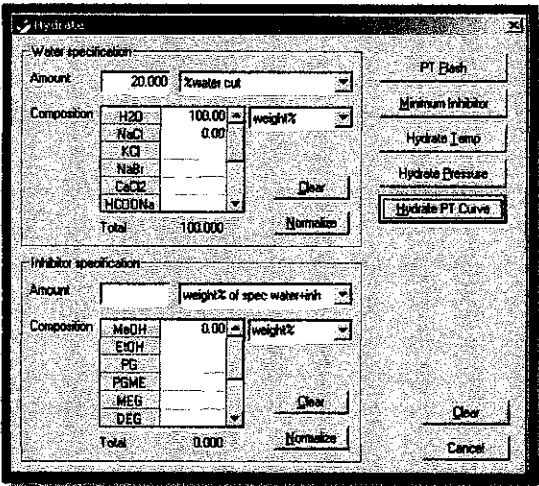


Figure C9: Simulation interface for hydrate

13. Graphical and numerical result will appear immediately.

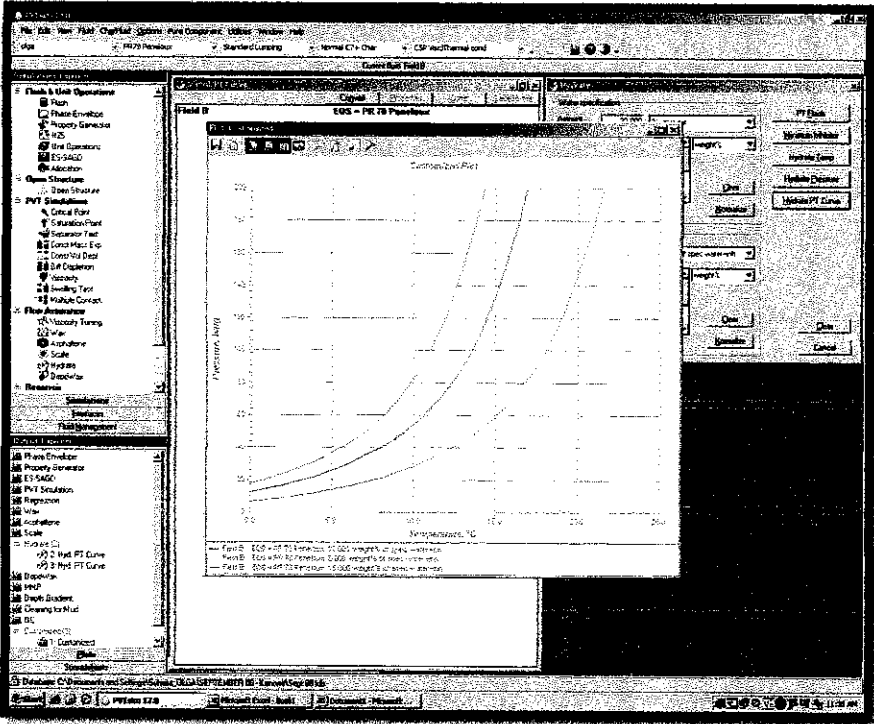


Figure C10: Graphical and numerical result of the simulation appeared immediately

APPENDIX D

RESULTS

Table D1: Hydrate phase boundary base case data for Field A and Field B

Base Case			
Field A		Field B	
T/°C	P/bar	T/°C	P/bar
0	6.37	0	6.83
1	7.35	1	7.85
2	8.49	2	9.03
3	9.80	3	10.39
4	11.31	4	11.96
5	13.06	5	13.76
6	15.07	6	15.83
7	17.40	7	18.21
8	20.09	8	20.95
9	23.19	9	24.11
10	26.77	10	27.74
11	30.91	11	31.92
12	35.69	12	36.73
13	41.21	13	42.26
14	47.58	14	48.63
15	54.95	15	55.97
16	63.46	16	64.41
17	73.29	17	74.13
18	84.64	18	85.33
19	97.77	19	98.21
20	112.93	20	113.05

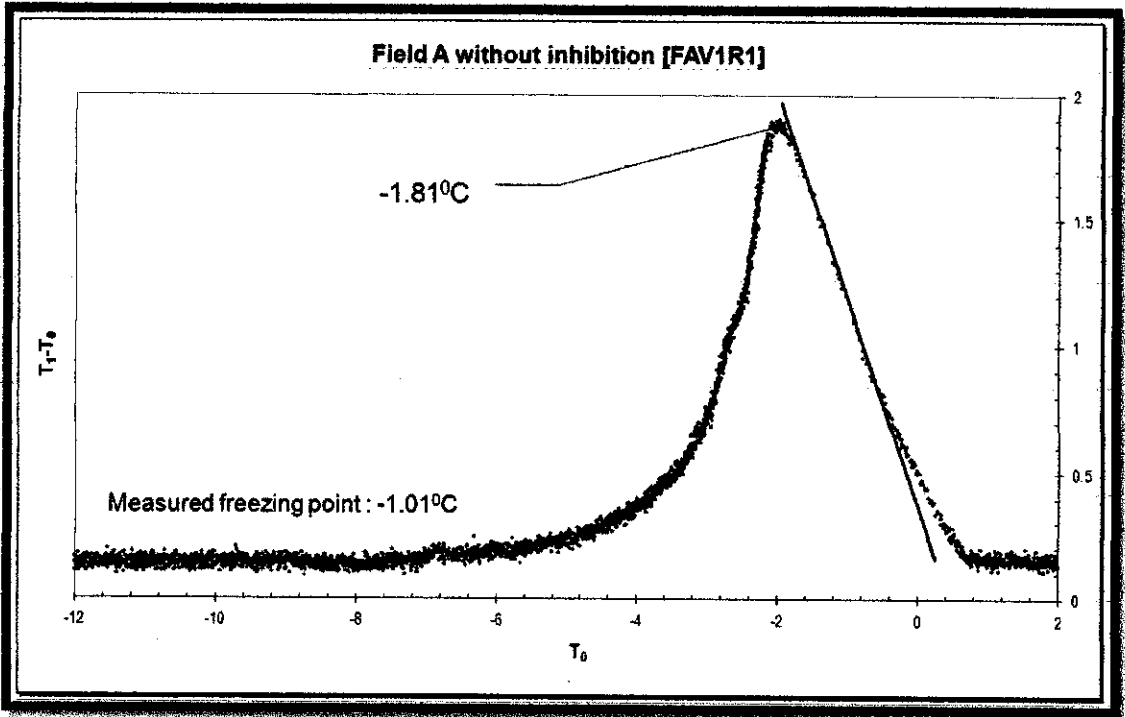


Figure D1: Freezing Point Depression Method - Field A without Inhibition (FAV1R1)

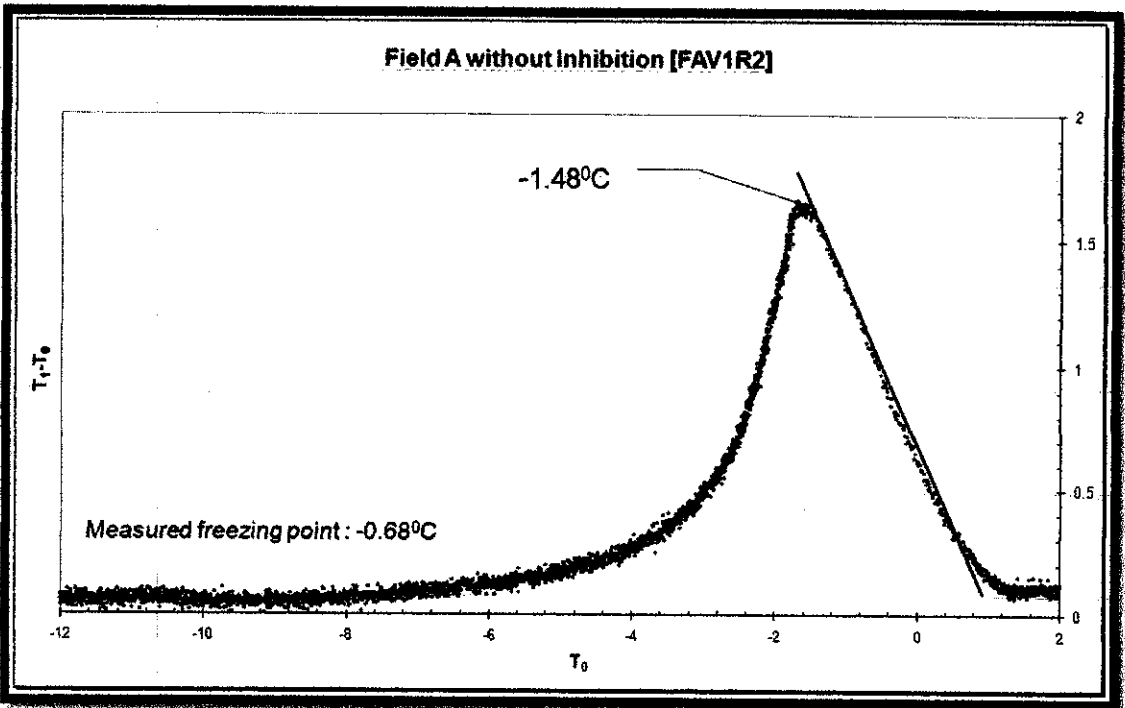


Figure D2: Freezing Point Depression Method - Field A without Inhibition (FAV1R2)

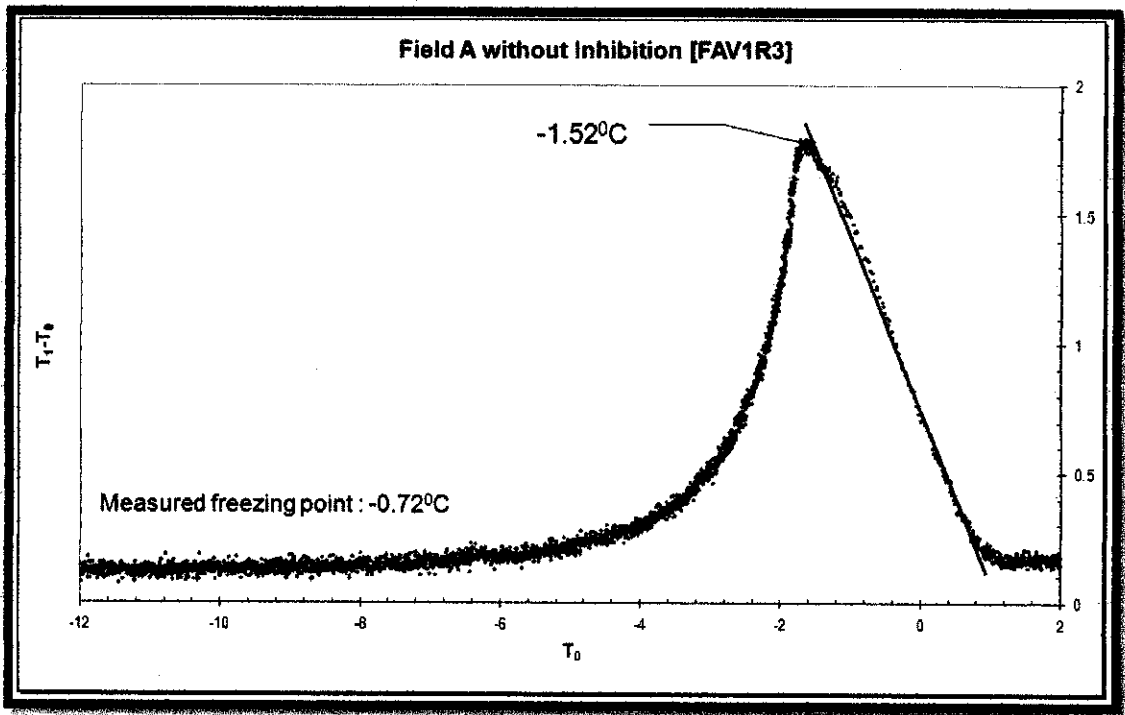


Figure D3: Freezing Point Depression Method - Field A without Inhibition (FAV1R3)

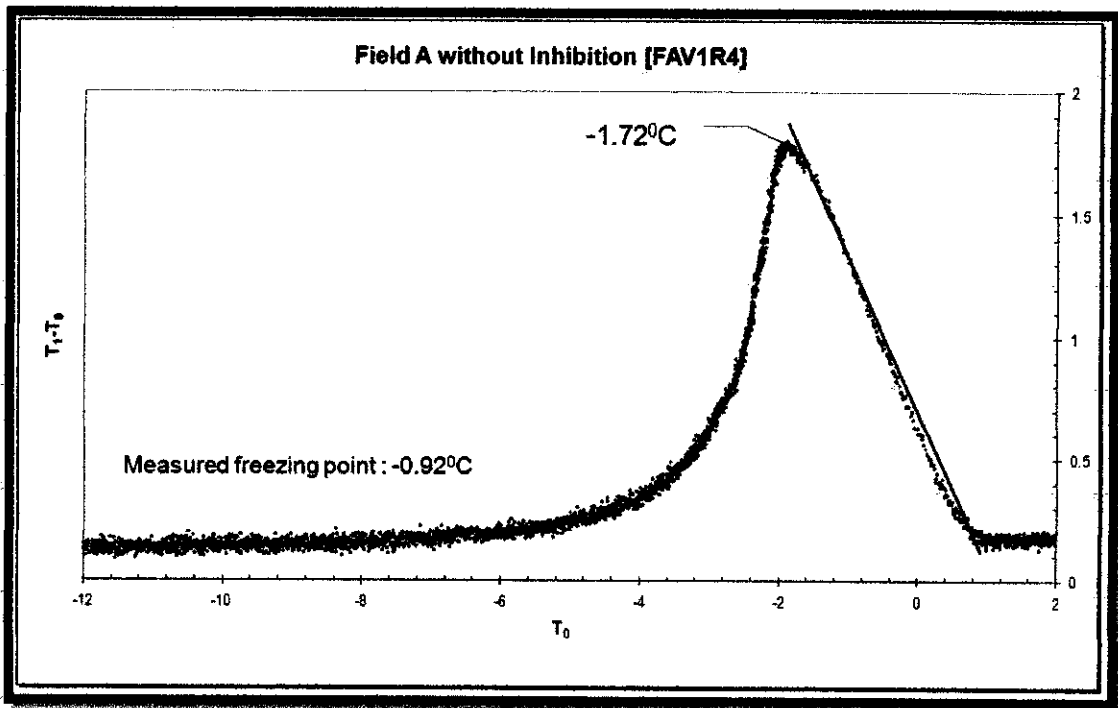


Figure D4: Freezing Point Depression Method - Field A without Inhibition (FAV1R4)

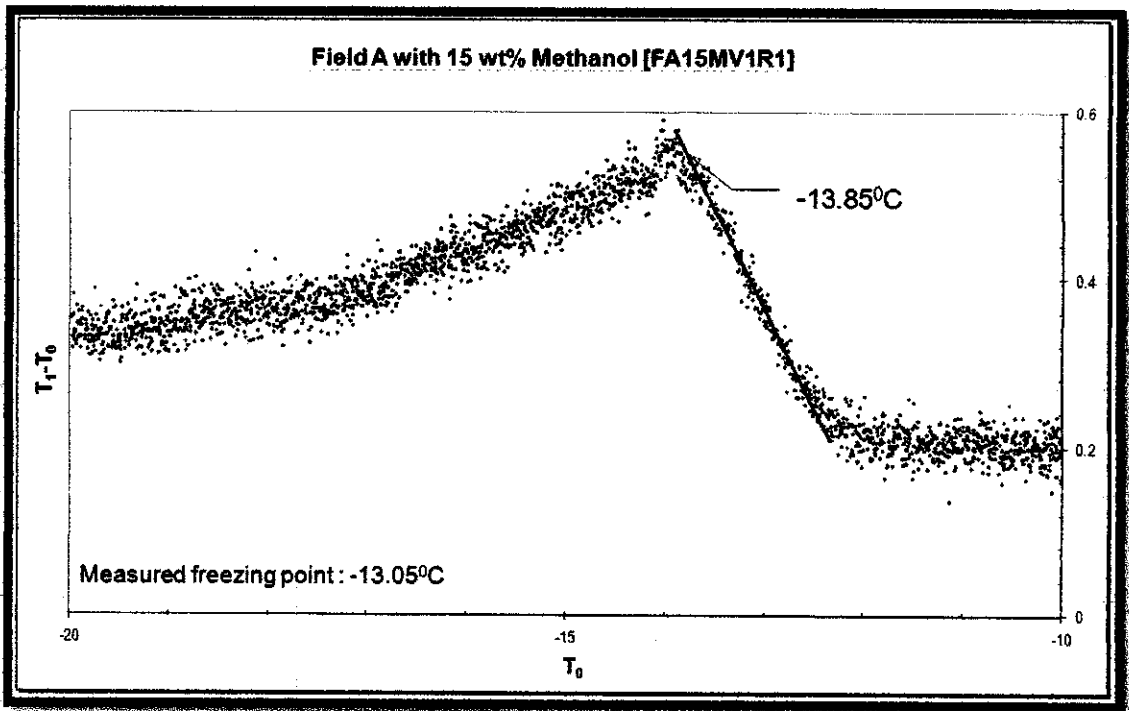


Figure D5: Freezing Point Depression Method - Field A with 15 wt% Methanol (FA15MV1R1)

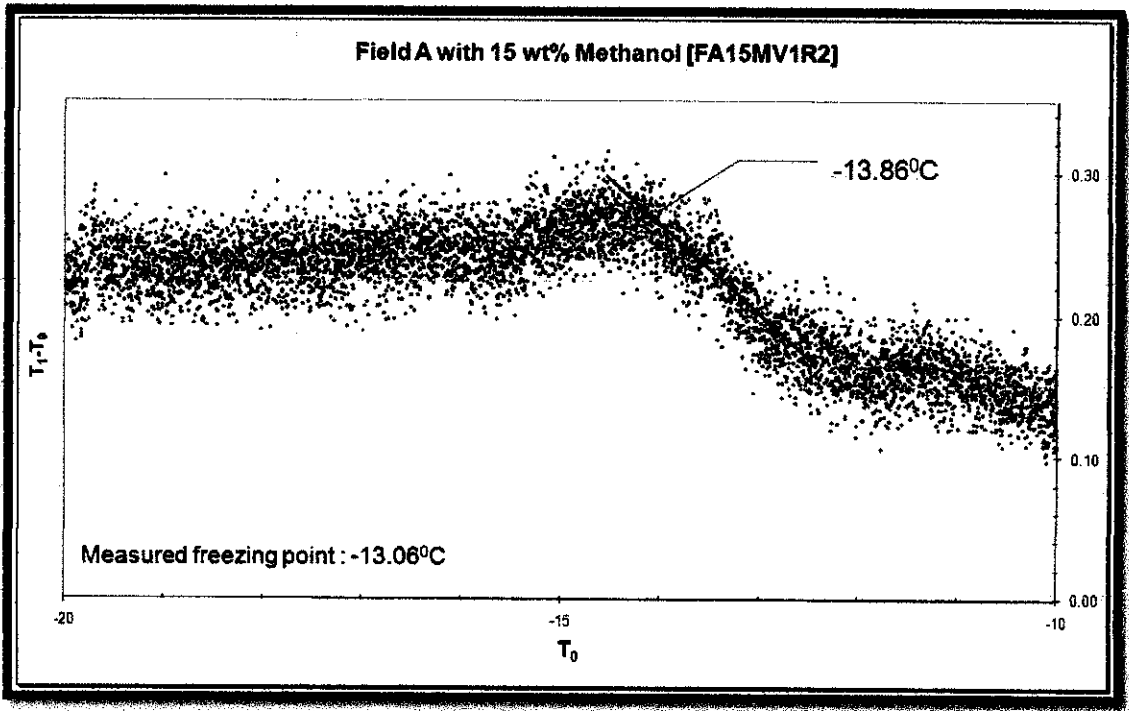


Figure D6: Freezing Point Depression Method - Field A with 15 wt% Methanol (FA15MV1R2)

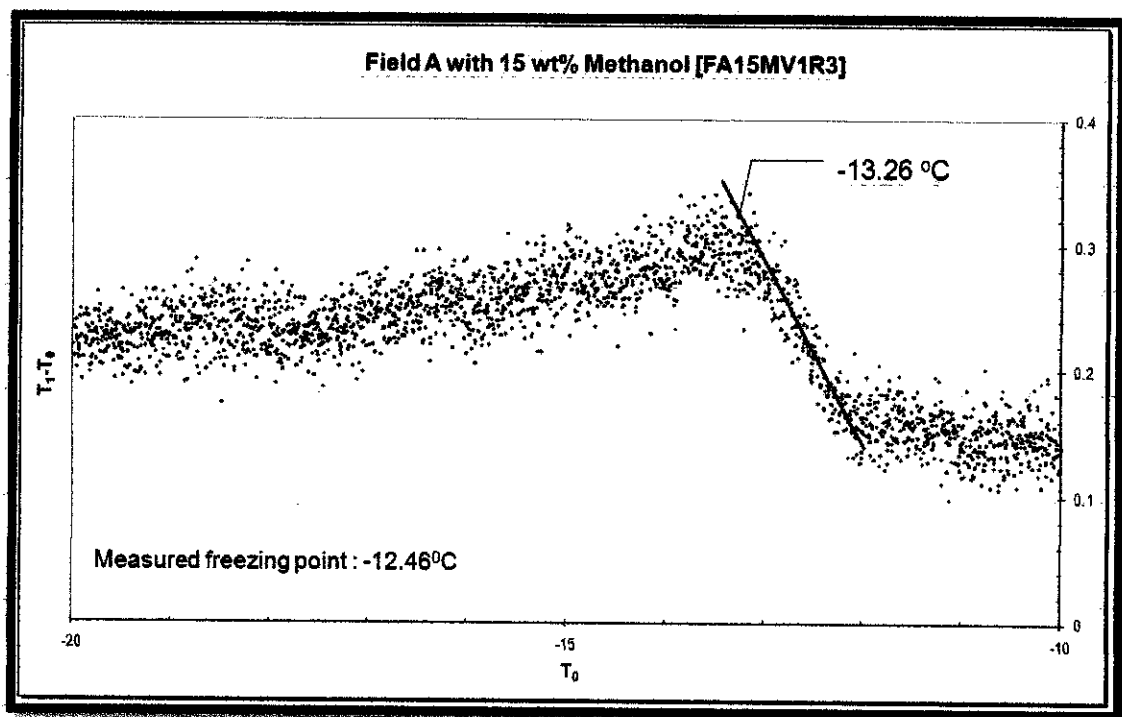


Figure D7: Freezing Point Depression Method - Field A with 15 wt% Methanol (FA15MV1R3)

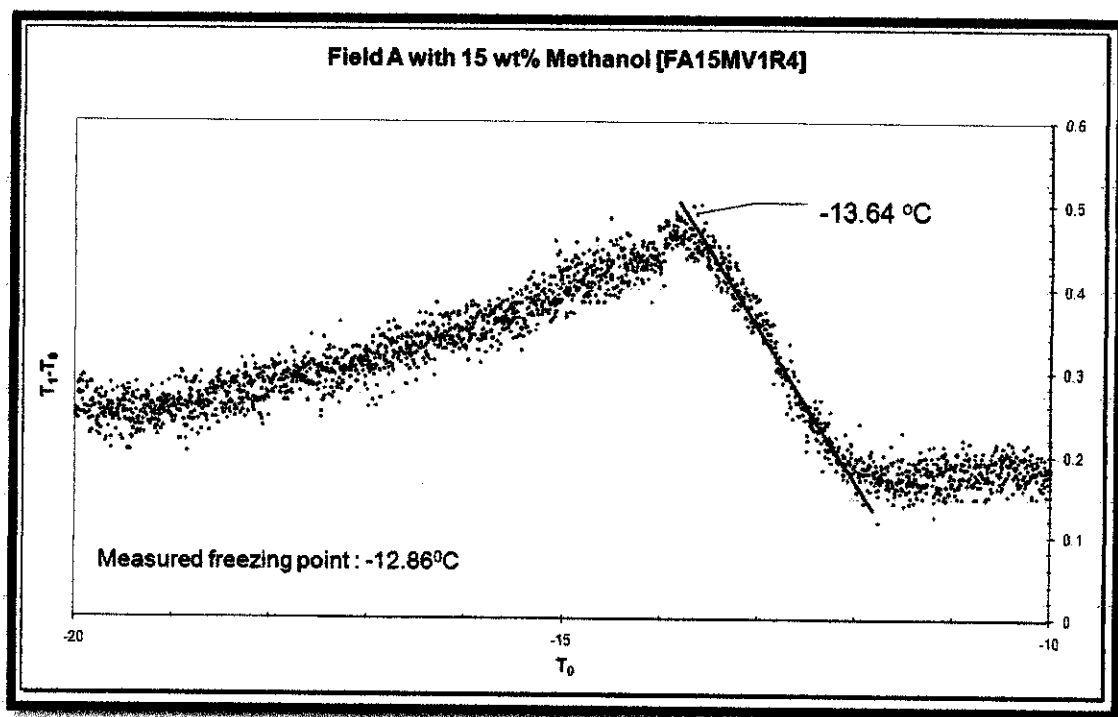


Figure D8: Freezing Point Depression Method - Field A with 15 wt% Methanol (FA15MV1R4)

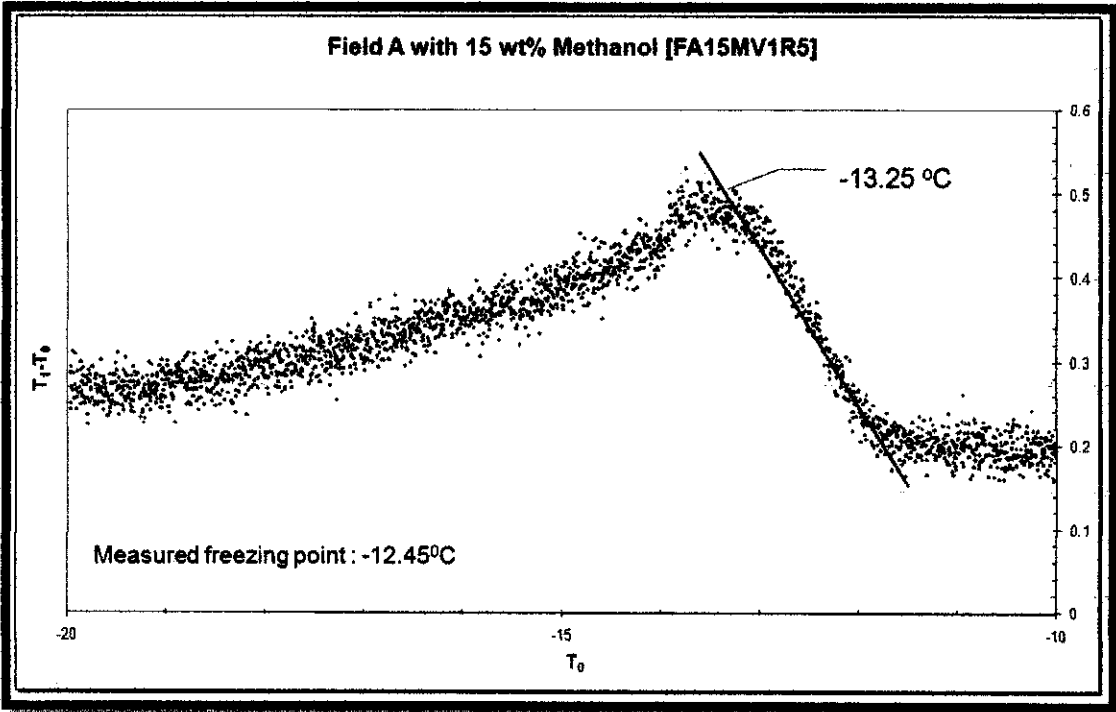


Figure D9: Freezing Point Depression Method - Field A with 15 wt% Methanol (FA15MV1R2)

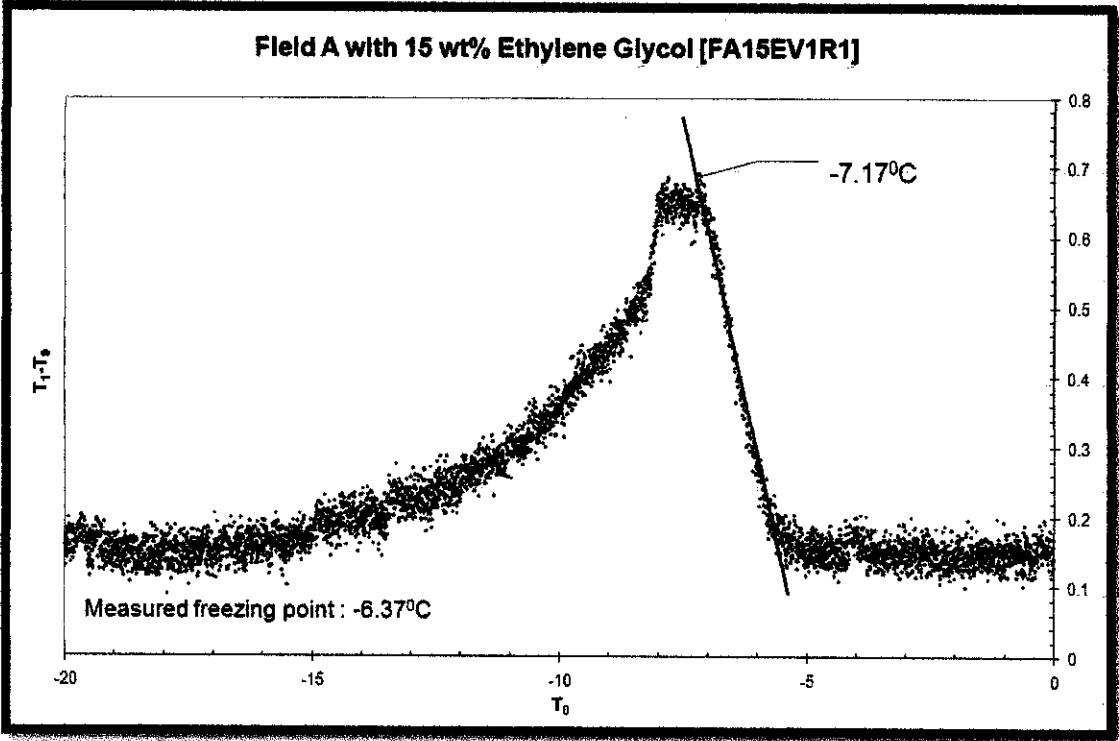


Figure D10: Freezing Point Depression Method - Field A with 15 wt% Ethylene Glycol (FA15EV1R1)

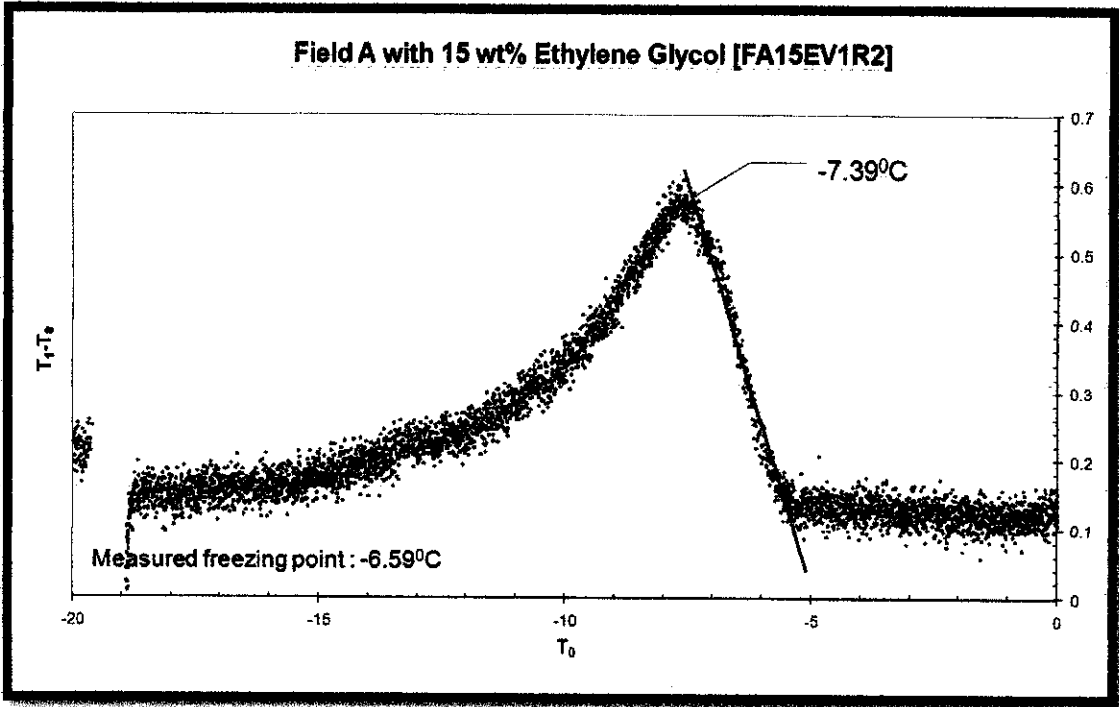


Figure D11: Freezing Point Depression Method - Field A with 15 wt% Ethylene Glycol (FA15EV1R2)

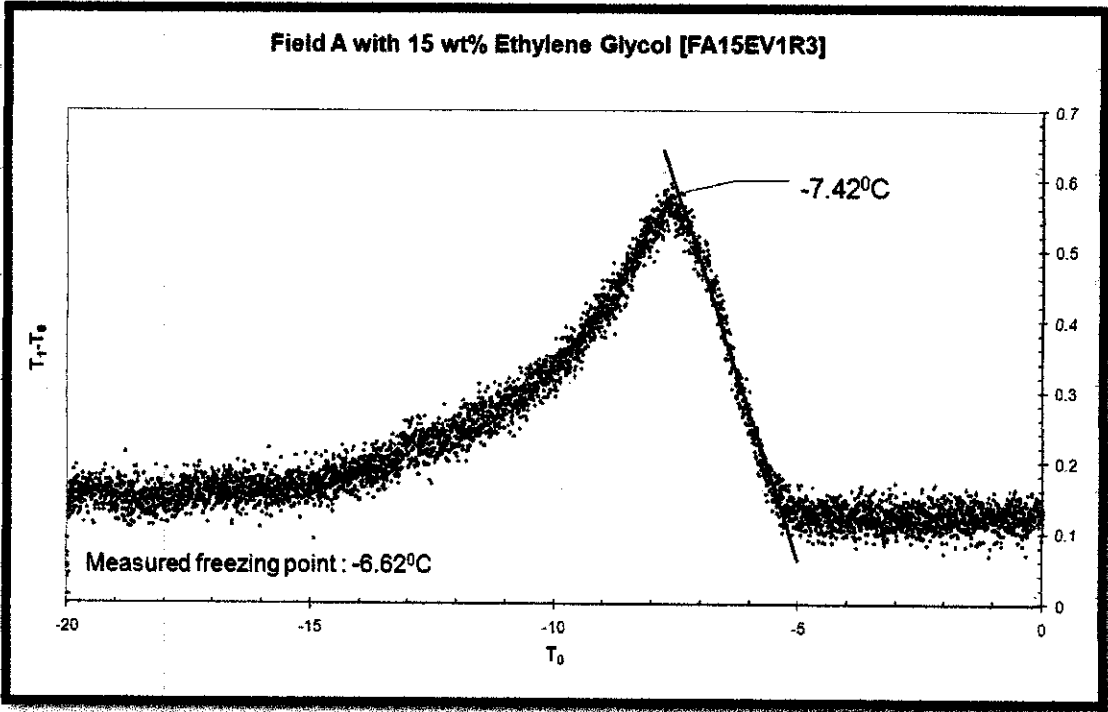


Figure D12: Freezing Point Depression Method - Field A with 15 wt% Ethylene Glycol (FA15EV1R3)

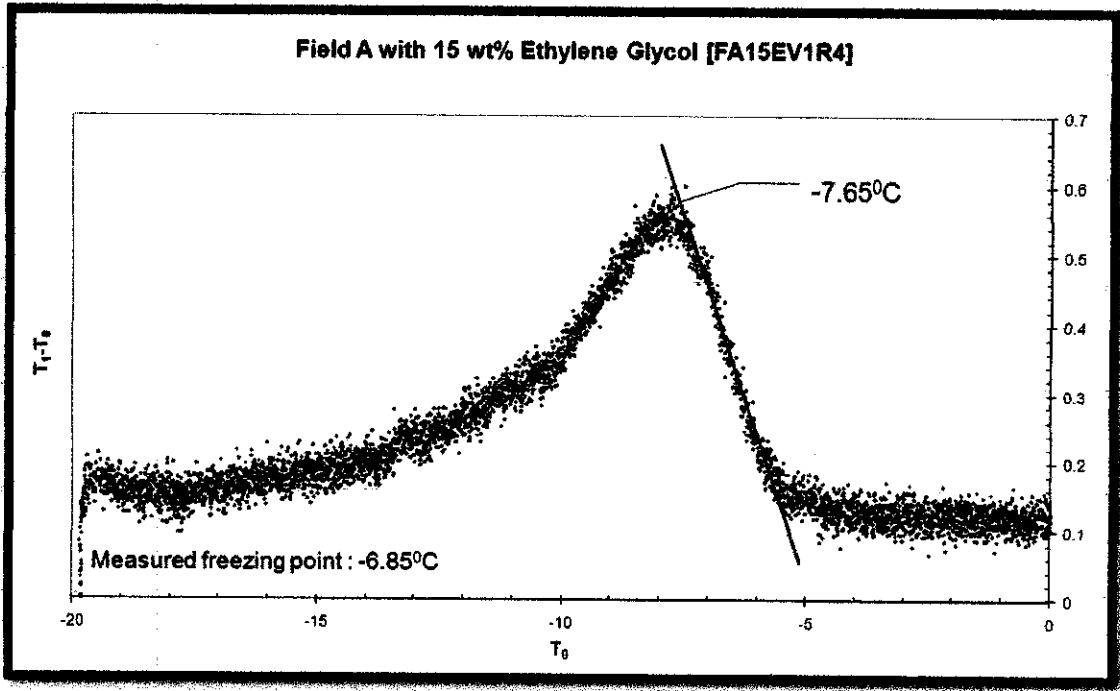


Figure D13: Freezing Point Depression Method - Field A with 15 wt% Ethylene Glycol (FA15EV1R4)

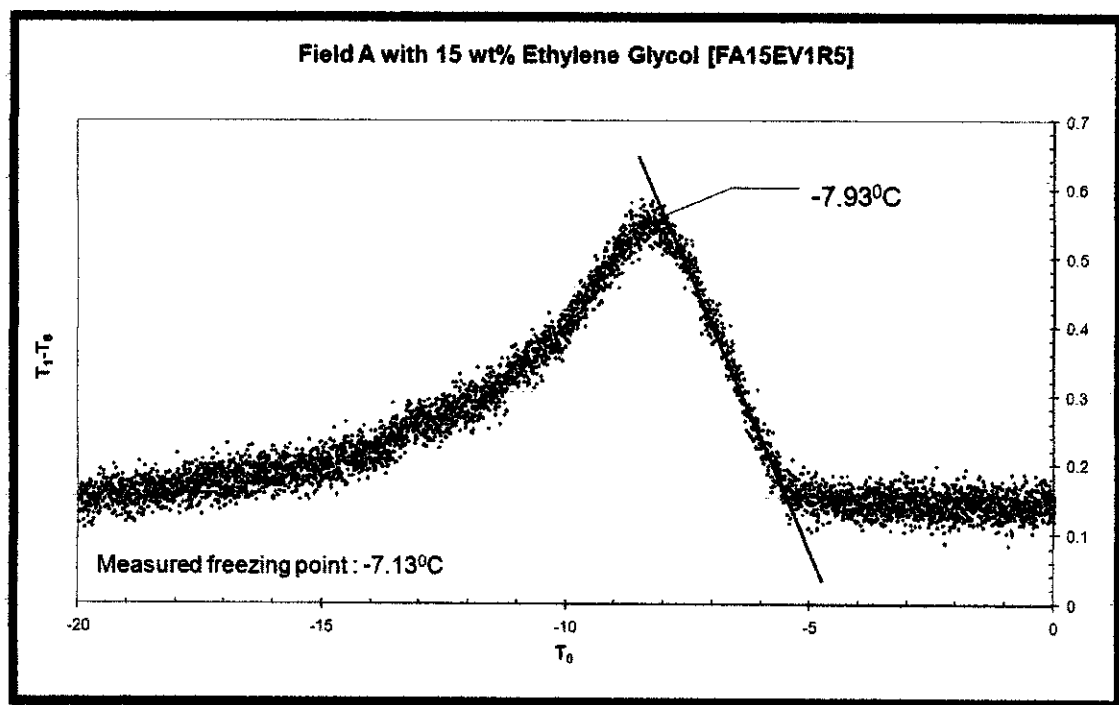


Figure D14: Freezing Point Depression Method - Field A with 15 wt% Ethylene Glycol (FA15EV1R5)

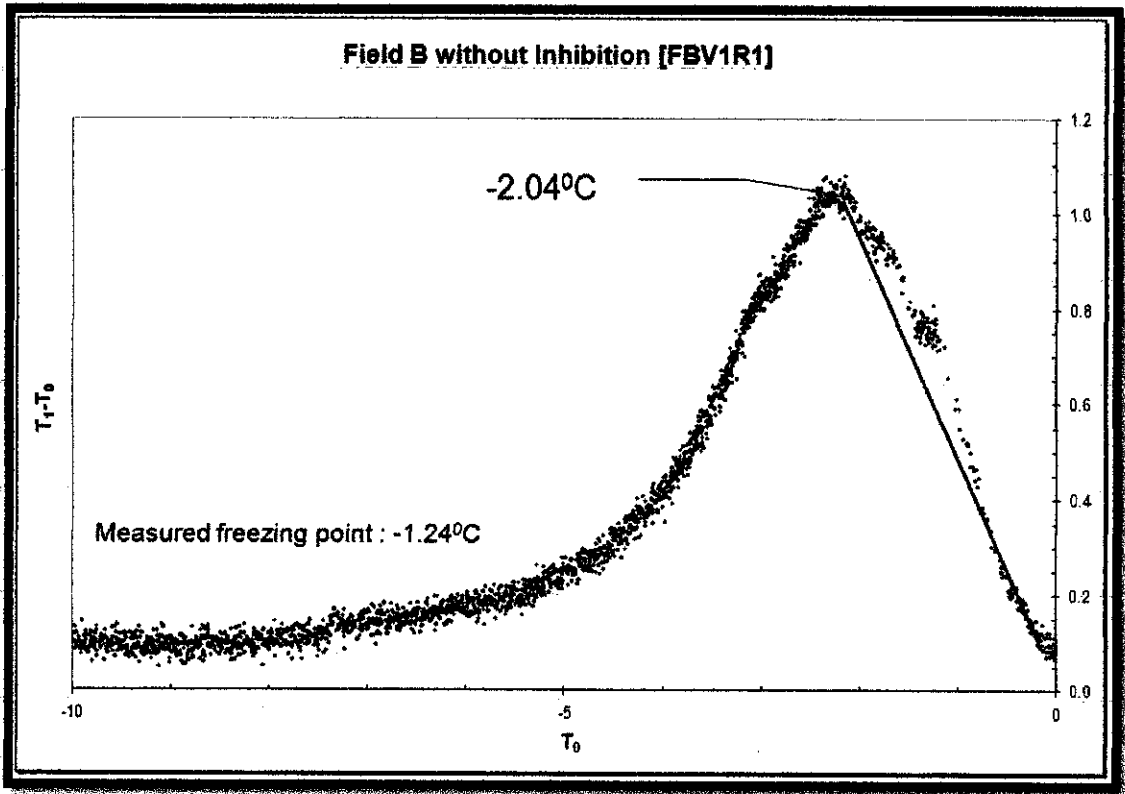


Figure D15: Freezing Point Depression Method - Field B without Inhibition (FBV1R1)

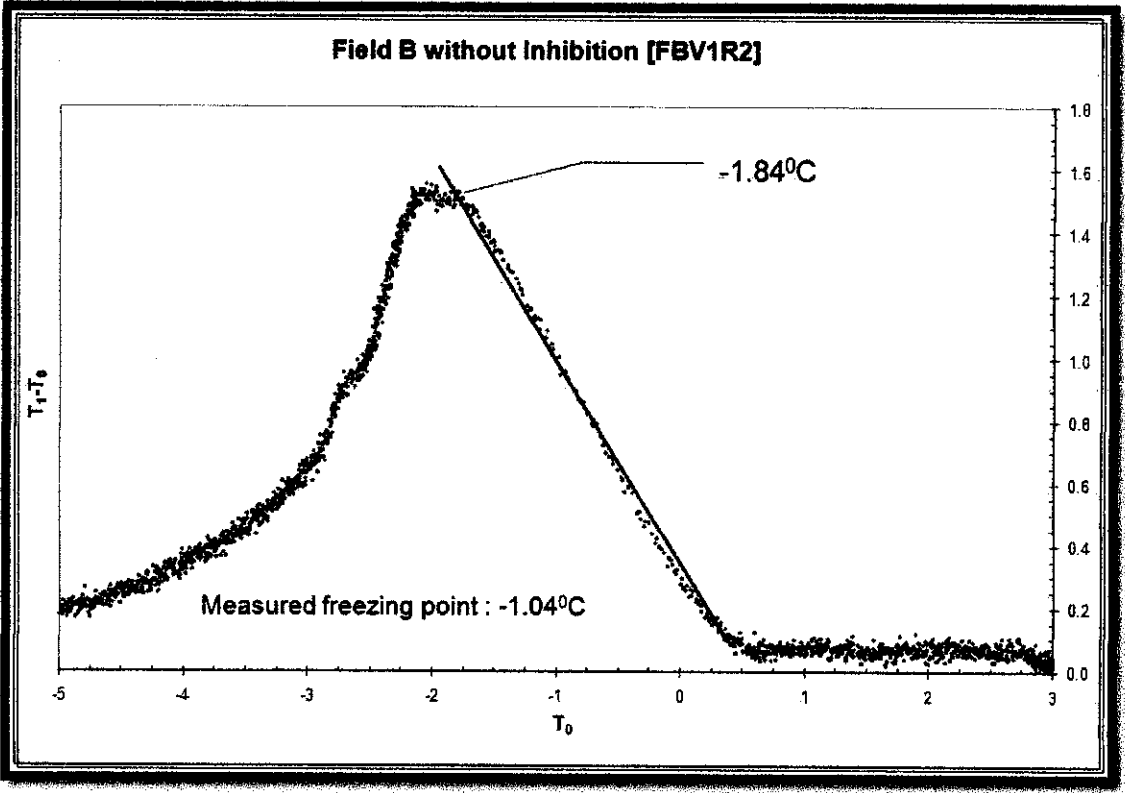


Figure D16: Freezing Point Depression Method - Field B without Inhibition (FBV1R2)

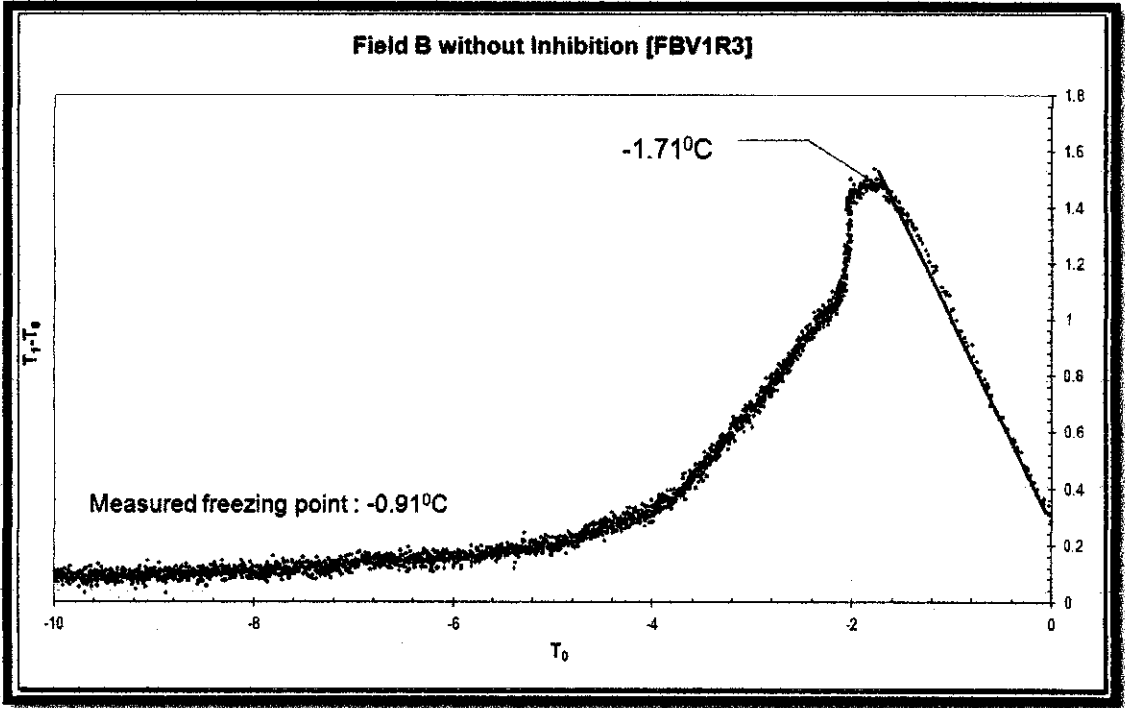


Figure D17: Freezing Point Depression Method - Field B without Inhibition (FBV1R3)

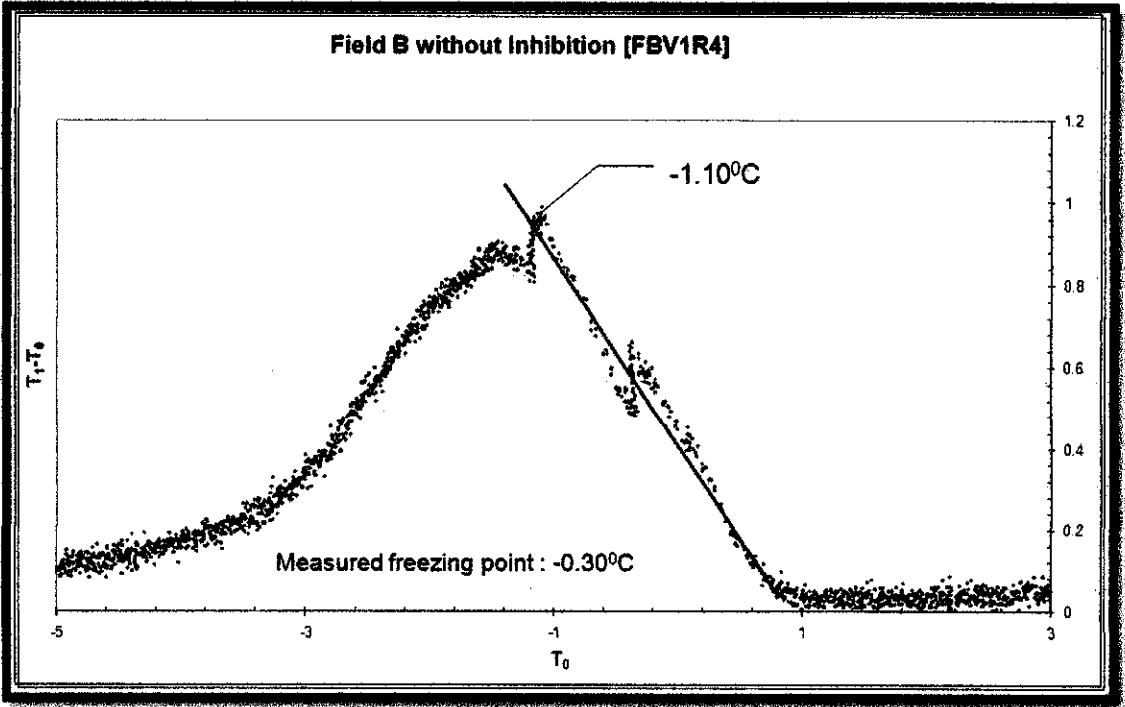


Figure D18: Freezing Point Depression Method - Field B without Inhibition (FBV1R4)

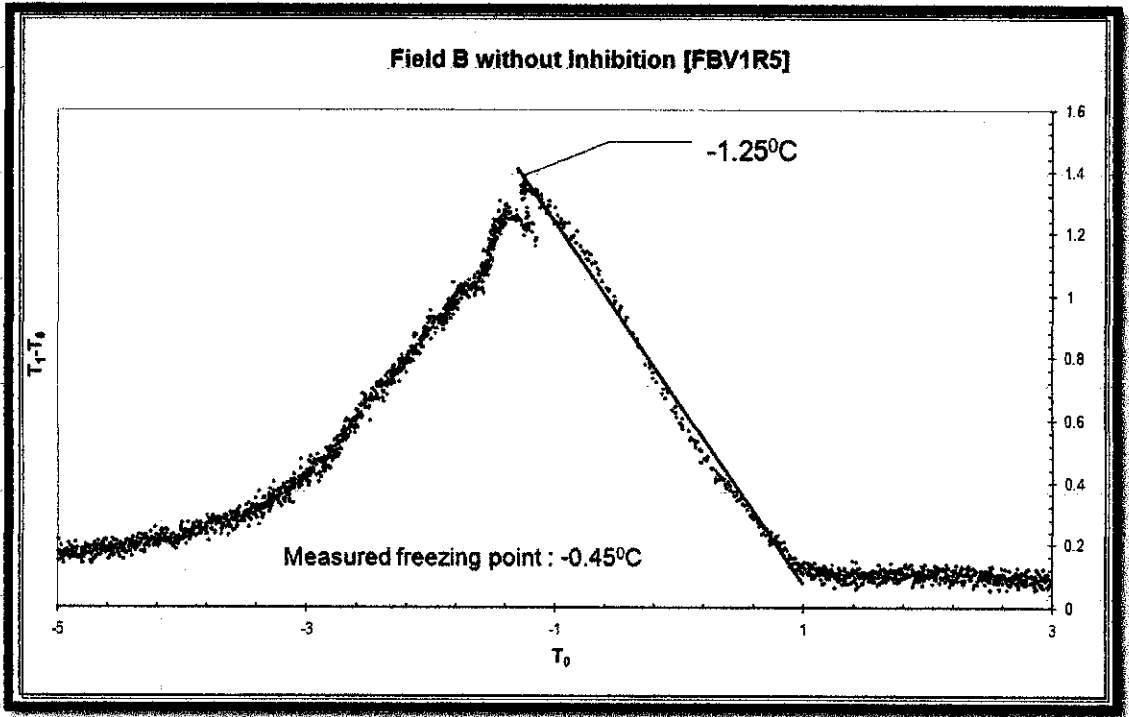


Figure D19: Freezing Point Depression Method - Field B without Inhibition (FBV1R5)

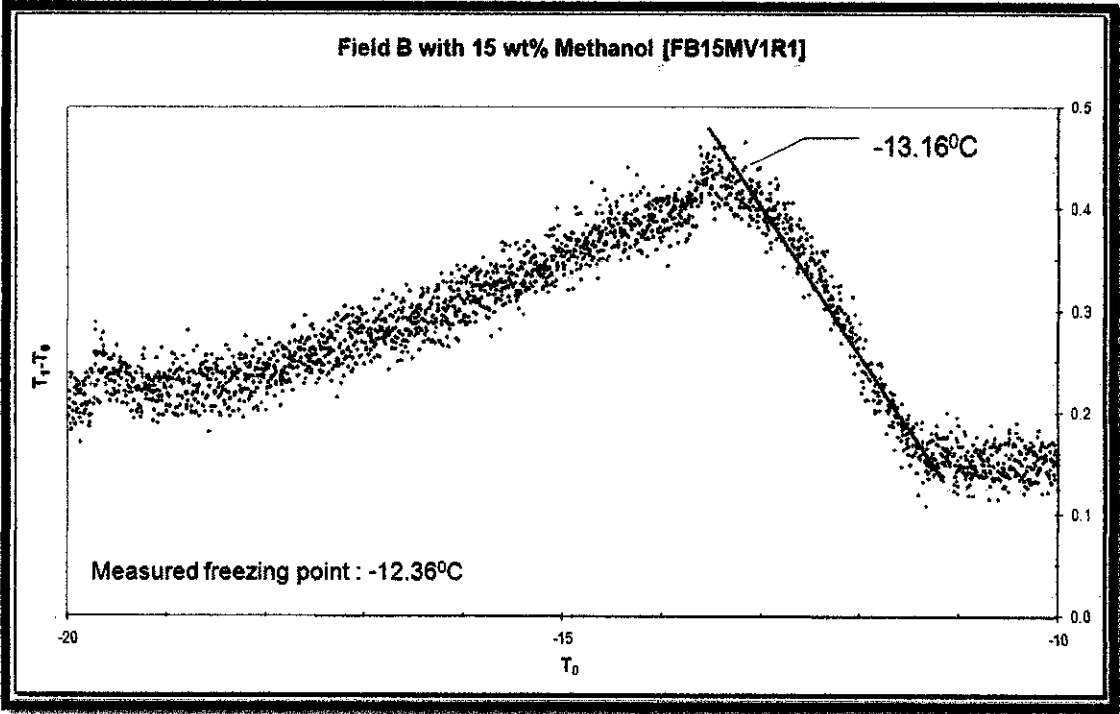


Figure D20: Freezing Point Depression Method - Field B with 15 wt% Methanol (FB15MV1R1)

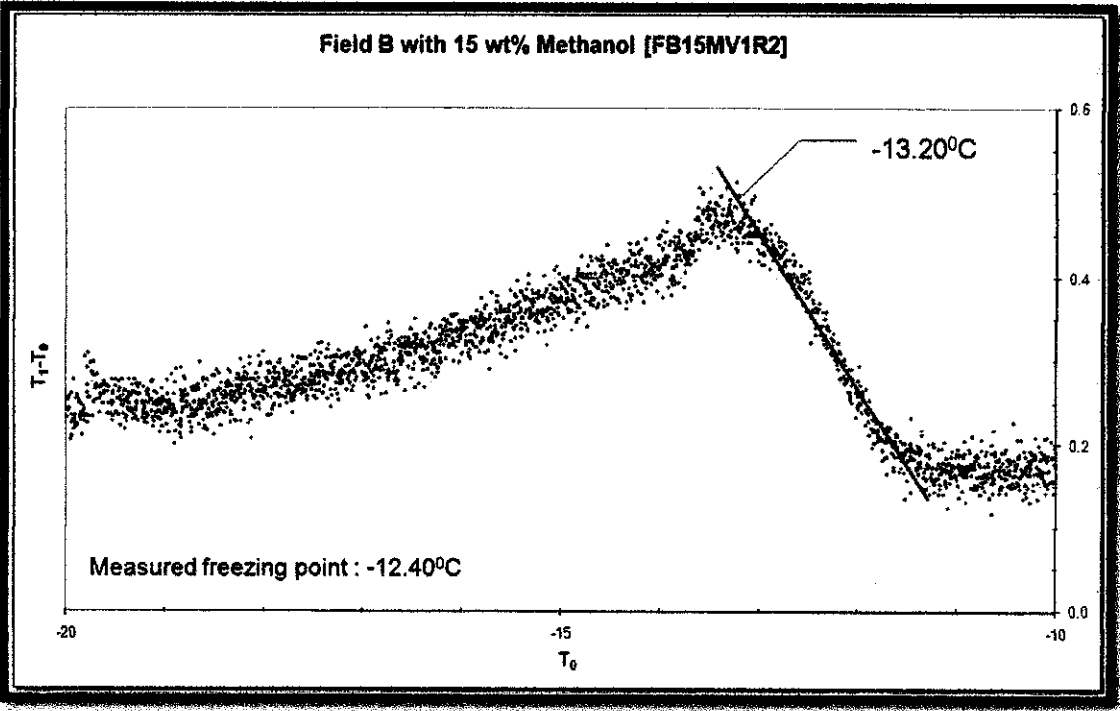


Figure D21: Freezing Point Depression Method - Field B with 15 wt% Methanol (FB15MV1R2)

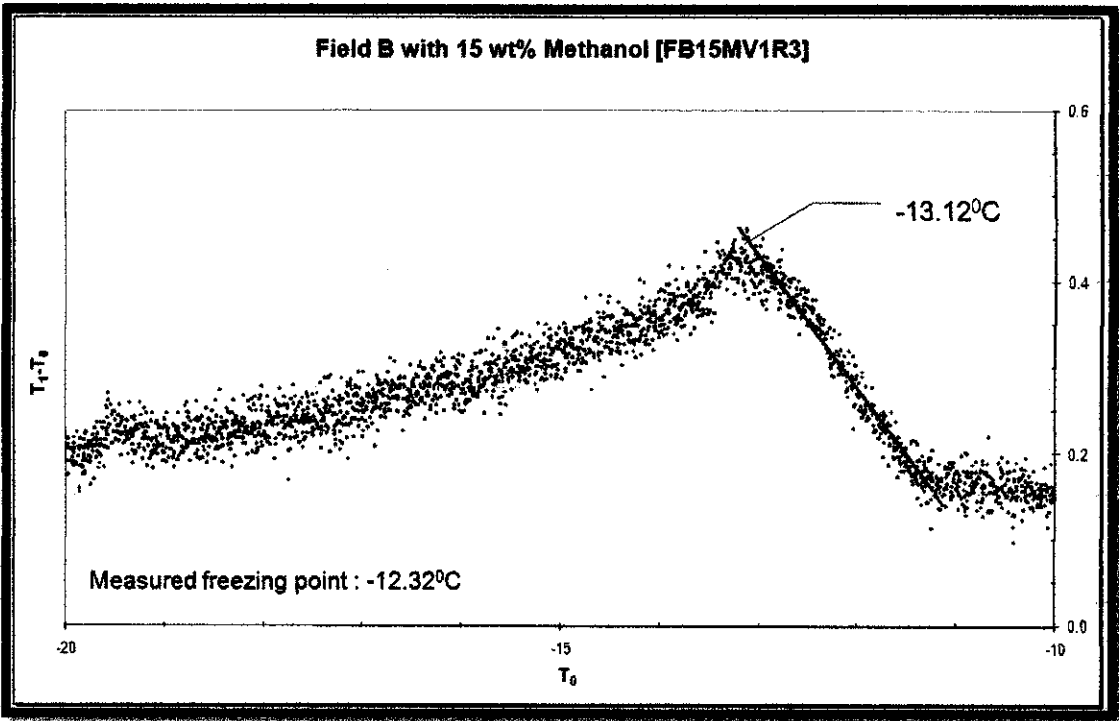


Figure D22: Freezing Point Depression Method - Field B with 15 wt% Methanol (FB15MV1R3)

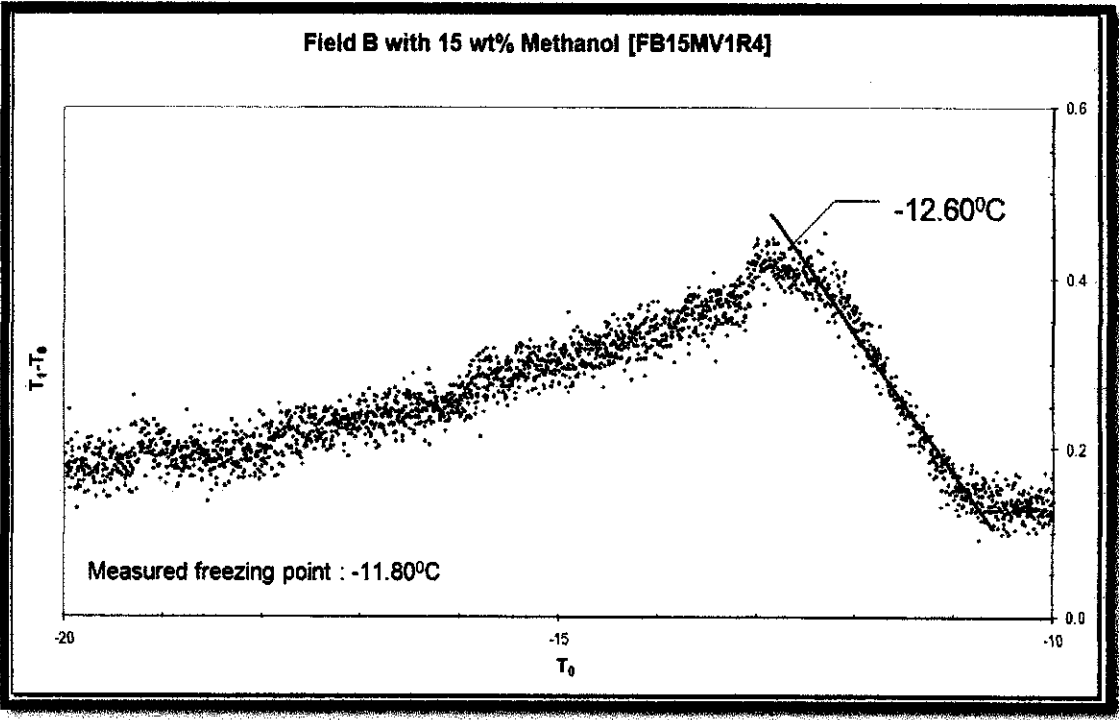


Figure D23: Freezing Point Depression Method - Field B with 15 wt% Methanol (FB15MV1R4)

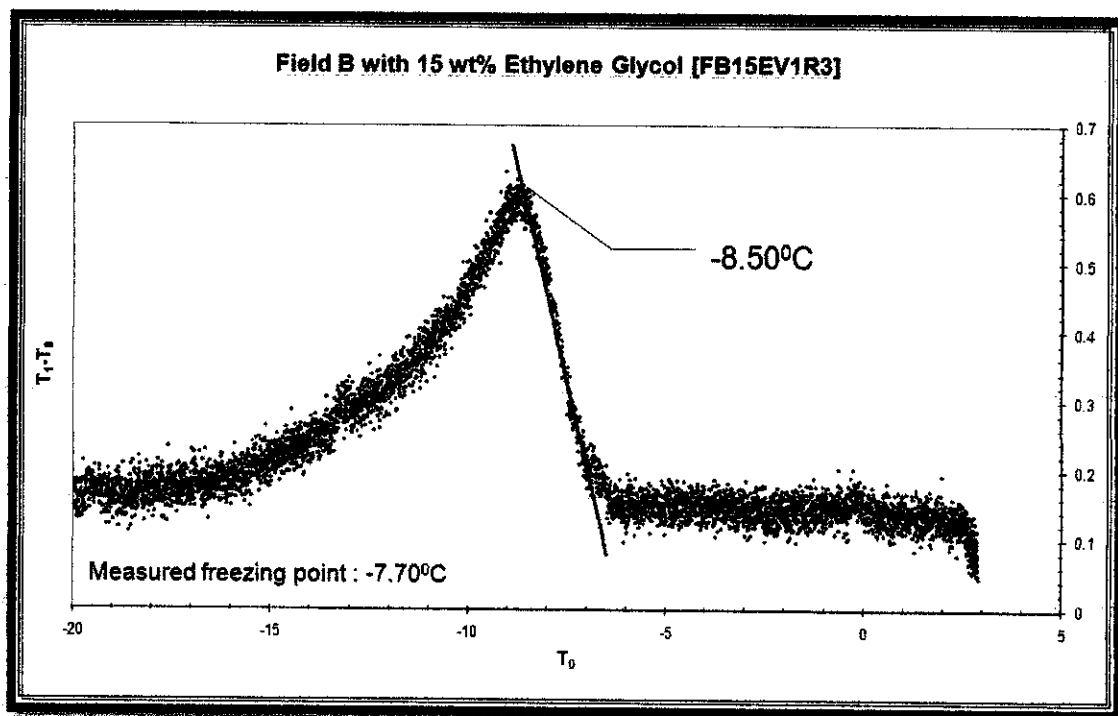


Figure D28: Freezing Point Depression Method - Field B with 15 wt% Ethylene Glycol (FB15EV1R3)

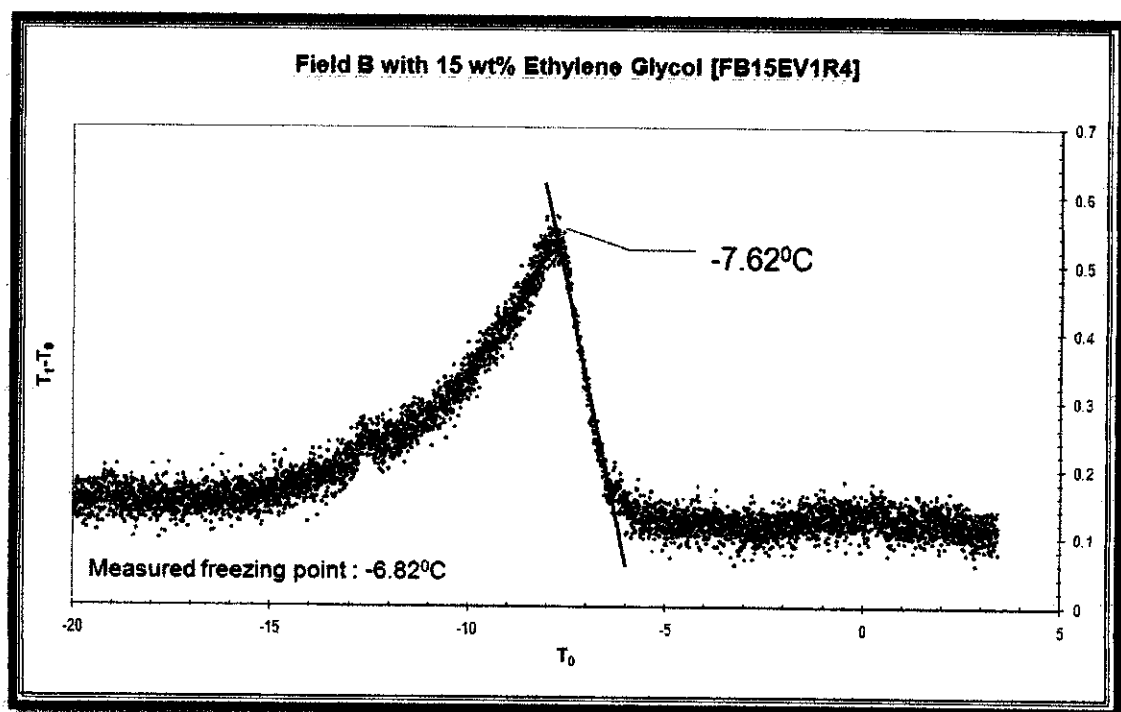


Figure D29: Freezing Point Depression Method - Field B with 15 wt% Ethylene Glycol (FB15EV1R4)

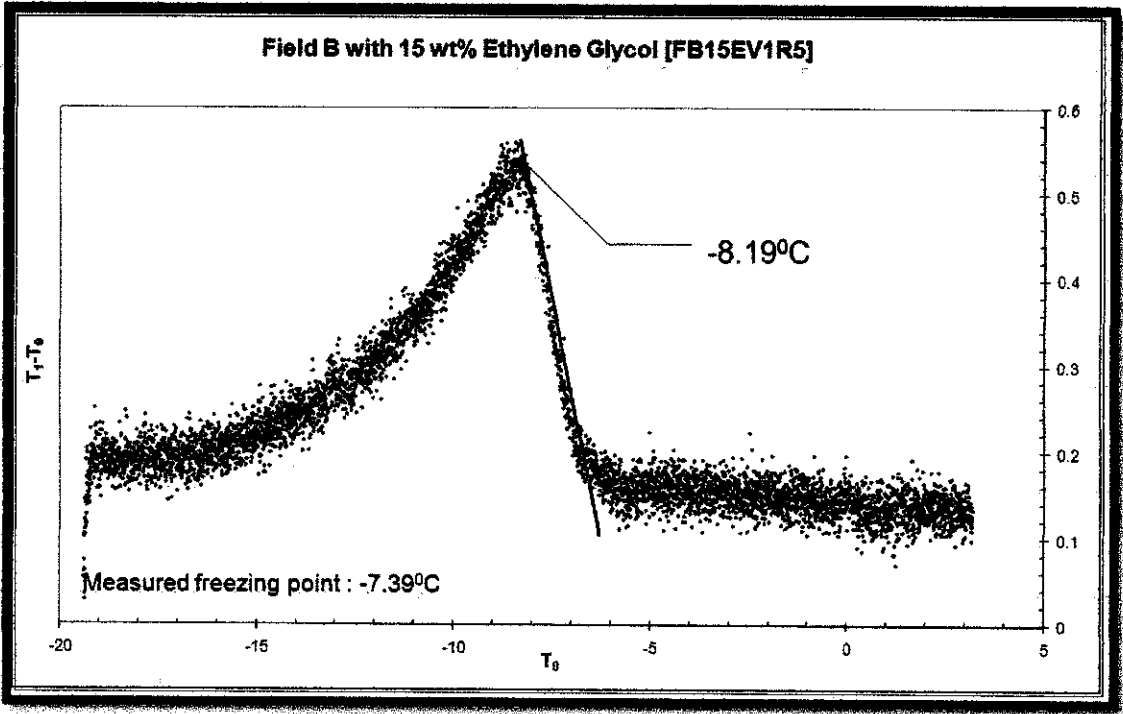


Figure D30: Freezing Point Depression Method - Field B with 15 wt% Ethylene Glycol (FB15EV1R5)

Table D2: C1 Correlation results for Field A with Methanol Inhibition

Correlation, $T = T_0 - 0.6825 \times \Delta T_f$					
Base case		Water sample without inhibition		Water sample with 15 wt% Methanol	
P_0/bar	$T_0/^{\circ}\text{C}$	$\Delta T_f/^{\circ}\text{C}$	$T/^{\circ}\text{C}$	$\Delta T_f/^{\circ}\text{C}$	$T/^{\circ}\text{C}$
6.37	0	0.83	-0.57	12.78	-8.72
7.35	1	0.83	0.43	12.78	-7.72
8.49	2	0.83	1.43	12.78	-6.72
9.80	3	0.83	2.43	12.78	-5.72
11.31	4	0.83	3.43	12.78	-4.72
13.06	5	0.83	4.43	12.78	-3.72
15.07	6	0.83	5.43	12.78	-2.72
17.40	7	0.83	6.43	12.78	-1.72
20.09	8	0.83	7.43	12.78	-0.72
23.19	9	0.83	8.43	12.78	0.28
26.77	10	0.83	9.43	12.78	1.28
30.91	11	0.83	10.43	12.78	2.28
35.69	12	0.83	11.43	12.78	3.28
41.21	13	0.83	12.43	12.78	4.28
47.58	14	0.83	13.43	12.78	5.28
54.95	15	0.83	14.43	12.78	6.28
63.46	16	0.83	15.43	12.78	7.28
73.29	17	0.83	16.43	12.78	8.28
84.64	18	0.83	17.43	12.78	9.28
97.77	19	0.83	18.43	12.78	10.28
112.93	20	0.83	19.43	12.78	11.28

Table D3: C2 Correlation results for Field A with Methanol Inhibition

Correlation, $T = T_0 - 0.5843 \times \Delta T_f \times P_0^{0.6435}$					
Base case		Water sample without inhibition		Water sample with 15 wt% Methanol	
P_0/bar	$T_0/^{\circ}\text{C}$	$\Delta T_f/^{\circ}\text{C}$	$T/^{\circ}\text{C}$	$\Delta T_f/^{\circ}\text{C}$	$T/^{\circ}\text{C}$
6.37	0	0.83	-0.53	12.78	-8.09
7.35	1	0.83	0.47	12.78	-7.14
8.49	2	0.83	1.47	12.78	-6.20
9.80	3	0.83	2.46	12.78	-5.25
11.31	4	0.83	3.46	12.78	-4.30
13.06	5	0.83	4.46	12.78	-3.35
15.07	6	0.83	5.45	12.78	-2.40
17.40	7	0.83	6.45	12.78	-1.46
20.09	8	0.83	7.45	12.78	-0.51
23.19	9	0.83	8.44	12.78	0.44
26.77	10	0.83	9.44	12.78	1.38
30.91	11	0.83	10.44	12.78	2.33
35.69	12	0.83	11.43	12.78	3.28
41.21	13	0.83	12.43	12.78	4.22
47.58	14	0.83	13.43	12.78	5.17
54.95	15	0.83	14.42	12.78	6.11
63.46	16	0.83	15.42	12.78	7.06
73.29	17	0.83	16.42	12.78	8.00
84.64	18	0.83	17.41	12.78	8.94
97.77	19	0.83	18.41	12.78	9.89
112.93	20	0.83	19.40	12.78	10.83

Table D4: C1 Correlation results for Field A with Ethylene Glycol Inhibition

Correlations, $T = T_0 - 0.6825 \times \Delta T_f$					
Base case		Water sample without inhibition		Water sample with 15 wt% Ethylene Glycol	
P_0/bar	$T_0/^{\circ}\text{C}$	$\Delta T_f/^{\circ}\text{C}$	$T/^{\circ}\text{C}$	$\Delta T_f/^{\circ}\text{C}$	$T/^{\circ}\text{C}$
6.37	0	0.83	-0.57	6.71	-4.58
7.35	1	0.83	0.43	6.71	-3.58
8.49	2	0.83	1.43	6.71	-2.58
9.80	3	0.83	2.43	6.71	-1.58
11.31	4	0.83	3.43	6.71	-0.58
13.06	5	0.83	4.43	6.71	0.42
15.07	6	0.83	5.43	6.71	1.42
17.40	7	0.83	6.43	6.71	2.42
20.09	8	0.83	7.43	6.71	3.42
23.19	9	0.83	8.43	6.71	4.42
26.77	10	0.83	9.43	6.71	5.42
30.91	11	0.83	10.43	6.71	6.42
35.69	12	0.83	11.43	6.71	7.42
41.21	13	0.83	12.43	6.71	8.42
47.58	14	0.83	13.43	6.71	9.42
54.95	15	0.83	14.43	6.71	10.42
63.46	16	0.83	15.43	6.71	11.42
73.29	17	0.83	16.43	6.71	12.42
84.64	18	0.83	17.43	6.71	13.42
97.77	19	0.83	18.43	6.71	14.42
112.93	20	0.83	19.43	6.71	15.42

Table D5: C2 Correlation results for Field A with Ethylene Glycol Inhibition

Correlations, $T = T_0 - 0.5843 \times \Delta T_f \times P_0^{0.0435}$					
Base case		Water sample without inhibition		Water sample with 15 wt% Ethylene Glycol	
P_0/bar	$T_0/^\circ\text{C}$	$\Delta T_f/^\circ\text{C}$	$T/^\circ\text{C}$	$\Delta T_f/^\circ\text{C}$	$T/^\circ\text{C}$
6.37	0	0.83	-0.53	6.71	-4.25
7.35	1	0.83	0.47	6.71	-3.28
8.49	2	0.83	1.47	6.71	-2.30
9.80	3	0.83	2.46	6.71	-1.33
11.31	4	0.83	3.46	6.71	-0.36
13.06	5	0.83	4.46	6.71	0.62
15.07	6	0.83	5.45	6.71	1.59
17.40	7	0.83	6.45	6.71	2.56
20.09	8	0.83	7.45	6.71	3.53
23.19	9	0.83	8.44	6.71	4.50
26.77	10	0.83	9.44	6.71	5.48
30.91	11	0.83	10.44	6.71	6.45
35.69	12	0.83	11.43	6.71	7.42
41.21	13	0.83	12.43	6.71	8.39
47.58	14	0.83	13.43	6.71	9.36
54.95	15	0.83	14.42	6.71	10.33
63.46	16	0.83	15.42	6.71	11.30
73.29	17	0.83	16.42	6.71	12.27
84.64	18	0.83	17.41	6.71	13.24
97.77	19	0.83	18.41	6.71	14.21
112.93	20	0.83	19.40	6.71	15.18

Table D6: C1 Correlation results for Field B with Methanol Inhibition

Correlation, $T = T_0 - 0.6825 \times \Delta T_f$					
Base case		Water sample without inhibition		Water sample with 15 wt% Methanol	
P_0/bar	$T_0/^\circ\text{C}$	$\Delta T_f/^\circ\text{C}$	$T/^\circ\text{C}$	$\Delta T_f/^\circ\text{C}$	$T/^\circ\text{C}$
6.83	0	0.79	-0.54	12.09	-8.25
7.85	1	0.79	0.46	12.09	-7.25
9.03	2	0.79	1.46	12.09	-6.25
10.39	3	0.79	2.46	12.09	-5.25
11.96	4	0.79	3.46	12.09	-4.25
13.76	5	0.79	4.46	12.09	-3.25
15.83	6	0.79	5.46	12.09	-2.25
18.21	7	0.79	6.46	12.09	-1.25
20.95	8	0.79	7.46	12.09	-0.25
24.11	9	0.79	8.46	12.09	0.75
27.74	10	0.79	9.46	12.09	1.75
31.92	11	0.79	10.46	12.09	2.75
36.73	12	0.79	11.46	12.09	3.75
42.26	13	0.79	12.46	12.09	4.75
48.63	14	0.79	13.46	12.09	5.75
55.97	15	0.79	14.46	12.09	6.75
64.41	16	0.79	15.46	12.09	7.75
74.13	17	0.79	16.46	12.09	8.75
85.33	18	0.79	17.46	12.09	9.75
98.21	19	0.79	18.46	12.09	10.75
113.05	20	0.79	19.46	12.09	11.75

Table D7: C2 Correlation results for Field B with Methanol Inhibition

Correlation, $T = T_0 - 0.5843 \times \Delta T_f \times P_0^{0.0435}$					
Base case		Water sample without inhibition		Water sample with 15 wt% Methanol	
P_0/bar	T_0/°C	ΔT_f/°C	T/°C	ΔT_f/°C	T/°C
6.83	0	0.79	-0.50	12.09	-7.68
7.85	1	0.79	0.50	12.09	-6.73
9.03	2	0.79	1.49	12.09	-5.77
10.39	3	0.79	2.49	12.09	-4.82
11.96	4	0.79	3.49	12.09	-3.87
13.76	5	0.79	4.48	12.09	-2.92
15.83	6	0.79	5.48	12.09	-1.97
18.21	7	0.79	6.48	12.09	-1.01
20.95	8	0.79	7.47	12.09	-0.06
24.11	9	0.79	8.47	12.09	0.89
27.74	10	0.79	9.47	12.09	1.84
31.92	11	0.79	10.46	12.09	2.79
36.73	12	0.79	11.46	12.09	3.74
42.26	13	0.79	12.46	12.09	4.69
48.63	14	0.79	13.45	12.09	5.64
55.97	15	0.79	14.45	12.09	6.58
64.41	16	0.79	15.45	12.09	7.53
74.13	17	0.79	16.44	12.09	8.48
85.33	18	0.79	17.44	12.09	9.43
98.21	19	0.79	18.44	12.09	10.38
113.05	20	0.79	19.43	12.09	11.32

Table D8: C1 Correlation results for Field B with Ethylene Glycol Inhibition

Correlations, $T = T_0 - 0.6825 \times \Delta T_f$					
Base case		Water sample without inhibition		Water sample with 15 wt% Ethylene Glycol	
P_0/bar	$T_0/^\circ\text{C}$	$\Delta T_f/^\circ\text{C}$	$T/^\circ\text{C}$	$\Delta T_f/^\circ\text{C}$	$T/^\circ\text{C}$
6.83	0	0.79	-0.54	7.38	-5.04
7.85	1	0.79	0.46	7.38	-4.04
9.03	2	0.79	1.46	7.38	-3.04
10.39	3	0.79	2.46	7.38	-2.04
11.96	4	0.79	3.46	7.38	-1.04
13.76	5	0.79	4.46	7.38	-0.04
15.83	6	0.79	5.46	7.38	0.96
18.21	7	0.79	6.46	7.38	1.96
20.95	8	0.79	7.46	7.38	2.96
24.11	9	0.79	8.46	7.38	3.96
27.74	10	0.79	9.46	7.38	4.96
31.92	11	0.79	10.46	7.38	5.96
36.73	12	0.79	11.46	7.38	6.96
42.26	13	0.79	12.46	7.38	7.96
48.63	14	0.79	13.46	7.38	8.96
55.97	15	0.79	14.46	7.38	9.96
64.41	16	0.79	15.46	7.38	10.96
74.13	17	0.79	16.46	7.38	11.96
85.33	18	0.79	17.46	7.38	12.96
98.21	19	0.79	18.46	7.38	13.96
113.05	20	0.79	19.46	7.38	14.96

Table D9: C2 Correlation results for Field B with Ethylene Glycol Inhibition

Correlations, $T = T_0 - 0.5843 \times \Delta T_f \times P_0^{0.0435}$					
Base case		Water sample without inhibition		Water sample with 15 wt% Ethylene Glycol	
P_0/bar	T_0/°C	ΔT_f/°C	T/°C	ΔT_f/°C	T/°C
6.83	0	0.79	-0.50	7.38	-4.69
7.85	1	0.79	0.50	7.38	-3.72
9.03	2	0.79	1.49	7.38	-2.75
10.39	3	0.79	2.49	7.38	-1.77
11.96	4	0.79	3.49	7.38	-0.80
13.76	5	0.79	4.48	7.38	0.17
15.83	6	0.79	5.48	7.38	1.14
18.21	7	0.79	6.48	7.38	2.11
20.95	8	0.79	7.47	7.38	3.08
24.11	9	0.79	8.47	7.38	4.05
27.74	10	0.79	9.47	7.38	5.02
31.92	11	0.79	10.46	7.38	5.99
36.73	12	0.79	11.46	7.38	6.96
42.26	13	0.79	12.46	7.38	7.93
48.63	14	0.79	13.45	7.38	8.89
55.97	15	0.79	14.45	7.38	9.86
64.41	16	0.79	15.45	7.38	10.83
74.13	17	0.79	16.44	7.38	11.80
85.33	18	0.79	17.44	7.38	12.77
98.21	19	0.79	18.44	7.38	13.74
113.05	20	0.79	19.43	7.38	14.70

Table D10: Simulation results for Field B in pure water sample

Pure water sample							
Without Inhibition		10 wt % Methanol		15 wt% Methanol		30 wt% Methanol	
T/°C	P/bar	T/°C	P/bar	T/°C	P/bar	T/°C	P/bar
-15.00	2.25	-15.00	2.25	-15.00	2.25	-15.00	6.30
-13.00	2.60	-13.00	2.60	-13.00	2.60	-13.00	8.63
-11.00	2.99	-11.00	2.99	-11.00	2.99	-11.00	11.70
-9.00	3.40	-9.00	3.40	-10.20	3.15	-9.00	15.75
-7.00	3.85	-7.00	3.85	-9.00	3.94	-7.00	21.19
-5.00	4.34	-6.47	3.98	-7.00	5.57	-5.00	28.59
-3.00	4.87	-5.00	5.15	-5.00	7.69	-3.05	38.59
-1.00	5.43	-3.00	7.14	-3.00	10.45	-1.62	48.59
-0.08	5.71	-1.00	9.73	-1.00	14.06	-0.51	58.59
1.00	6.81	1.00	13.10	1.00	18.82	0.38	68.59
3.00	9.29	3.00	17.53	3.00	25.17	1.11	78.59
5.00	12.50	5.00	23.39	5.00	33.78	1.72	88.59
7.00	16.69	7.00	31.28	6.71	43.78	2.25	98.59
9.00	22.20	8.87	41.28	8.02	53.78	2.70	108.59
11.00	29.54	10.28	51.28	9.07	63.78	3.10	118.59
13.00	39.47	11.40	61.28	9.92	73.78	3.46	128.59
14.52	49.47	12.31	71.28	10.64	83.78	3.79	138.59
15.71	59.47	13.07	81.28	11.25	93.78	4.09	148.59
16.68	69.47	13.72	91.28	11.78	103.78	4.36	158.59
17.50	79.47	14.28	101.28	12.24	113.78	4.62	168.59
18.19	89.47	14.77	111.28	12.66	123.78	4.87	178.59
18.78	99.47	15.21	121.28	13.03	133.78	5.10	188.59
19.31	109.47	15.60	131.28	13.37	143.78	5.33	198.59
19.77	119.47	15.96	141.28	13.68	153.78	5.54	198.99
20.19	129.47	16.29	151.28	13.98	163.78		
20.56	139.47	16.59	161.28	14.25	173.78		
20.91	149.47	16.87	171.28	14.51	183.78		
21.23	159.47	17.14	181.28	14.75	193.78		
21.53	169.47	17.39	191.28	14.87	198.99		
21.81	179.47	17.58	198.99				
22.07	189.47						
22.31	198.99						

Table D11: Simulation results for Field B in 1.7 wt% NaCl water sample

Field B water sample (1.7 wt% NaCl)							
Without Inhibition		10 wt % Methanol		15 wt% Methanol		30 wt% Methanol	
T/°C	P/bar	T/°C	P/bar	T/°C	P/bar	T/°C	P/bar
-15.00	2.25	-15.00	2.25	-15.00	2.25	-15.00	6.47
-13.00	2.60	-13.00	2.60	-13.00	2.60	-13.00	8.86
-11.00	2.99	-11.00	2.99	-11.00	2.99	-11.00	12.00
-9.00	3.40	-9.00	3.40	-10.98	2.99	-9.00	16.17
-7.00	3.85	-7.37	3.77	-9.00	4.32	-7.00	21.77
-5.00	4.34	-7.00	4.03	-7.00	6.06	-5.00	29.42
-3.00	4.87	-5.00	5.69	-5.00	8.33	-3.12	39.42
-1.09	5.41	-3.00	7.85	-3.00	11.28	-1.72	49.42
-1.00	5.49	-1.00	10.65	-1.00	15.16	-0.64	59.42
1.00	7.58	1.00	14.31	1.00	20.29	0.23	69.42
3.00	10.30	3.00	19.14	3.00	27.18	0.95	79.42
5.00	13.83	5.00	25.56	5.00	36.58	1.55	89.42
7.00	18.44	7.00	34.26	6.57	46.58	2.06	99.42
9.00	24.54	8.70	44.26	7.79	56.58	2.51	109.42
11.00	32.72	10.01	54.26	8.77	66.58	2.90	119.42
12.82	42.72	11.05	64.26	9.58	76.58	3.25	129.42
14.21	52.72	11.91	74.26	10.26	86.58	3.57	139.42
15.31	62.72	12.63	84.26	10.84	96.58	3.87	149.42
16.22	72.72	13.25	94.26	11.35	106.58	4.14	159.42
16.99	82.72	13.78	104.26	11.79	116.58	4.39	169.42
17.64	92.72	14.25	114.26	12.19	126.58	4.64	179.42
18.20	102.72	14.67	124.26	12.55	136.58	4.87	189.42
18.70	112.72	15.05	134.26	12.88	146.58	5.08	198.99
19.15	122.72	15.39	144.26	13.19	156.58		
19.54	132.72	15.71	154.26	13.47	166.58		
19.91	142.72	16.00	164.26	13.74	176.58		
20.24	152.72	16.28	174.26	13.99	186.58		
20.55	162.72	16.54	184.26	14.23	196.58		
20.84	172.72	16.78	194.26	14.28	198.99		
21.11	182.72	16.90	198.99				
21.37	192.72						
21.52	198.99						

Table D12: Simulation results for Field B in 1.5 wt% NaCl water sample

Field B water sample (1.5 wt% NaCl)							
Without Inhibition		10 wt % Methanol		15 wt% Methanol		30 wt% Methanol	
T/°C	P/bar	T/°C	P/bar	T/°C	P/bar	T/°C	P/bar
-15.00	2.25	-15.00	2.25	-15.00	2.25	-15.00	6.43
-13.00	2.60	-13.00	2.60	-13.00	2.60	-13.00	8.81
-11.00	2.99	-11.00	2.99	-11.00	2.99	-11.00	11.94
-9.00	3.40	-9.00	3.40	-10.88	3.01	-9.00	16.09
-7.00	3.85	-7.27	3.79	-9.00	4.27	-7.00	21.66
-5.00	4.34	-7.00	3.98	-7.00	6.00	-5.00	29.27
-3.00	4.87	-5.00	5.63	-5.00	8.25	-3.10	39.27
-1.00	5.43	-3.00	7.76	-3.00	11.18	-1.70	49.27
-0.97	5.44	-1.00	10.54	-1.00	15.02	-0.62	59.27
1.00	7.49	1.00	14.16	1.00	20.10	0.26	69.27
3.00	10.18	3.00	18.93	3.00	26.91	0.97	79.27
5.00	13.67	5.00	25.29	5.00	36.21	1.58	89.27
7.00	18.23	7.00	33.88	6.59	46.21	2.09	99.27
9.00	24.26	8.72	43.88	7.82	56.21	2.54	109.27
11.00	32.33	10.04	53.88	8.81	66.21	2.93	119.27
12.84	42.33	11.10	63.88	9.62	76.21	3.29	129.27
14.24	52.33	11.96	73.88	10.31	86.21	3.61	139.27
15.36	62.33	12.68	83.88	10.89	96.21	3.90	149.27
16.28	72.33	13.30	93.88	11.40	106.21	4.18	159.27
17.05	82.33	13.84	103.88	11.85	116.21	4.43	169.27
17.70	92.33	14.31	113.88	12.25	126.21	4.68	179.27
18.27	102.33	14.73	123.88	12.61	136.21	4.91	189.27
18.77	112.33	15.11	133.88	12.94	146.21	5.13	198.99
19.22	122.33	15.46	143.88	13.25	156.21		
19.62	132.33	15.78	153.88	13.53	166.21		
19.98	142.33	16.07	163.88	13.80	176.21		
20.32	152.33	16.35	173.88	14.05	186.21		
20.63	162.33	16.61	183.88	14.29	196.21		
20.92	172.33	16.86	193.88	14.36	198.99		
21.19	182.33	16.98	198.99				
21.45	192.33						
21.61	198.99						